Motahareh Safari, B.Sc

Production of Agrin22 and Agrin15 overexpression AAV and their validation *in vitro* to check the effect of these fragments in synapses

MASTER'S THESIS

to achieve the university degree of
Biotechnology

Submitted to
Graz University of Technology

Home supervisor: Assoz.Prof.Mag.Dr.rer.nat Manfred Hartbauer
Name of institute: Institute of Biology, University of Graz

Host supervisor: Prof. Alexander Dityatev
Name of institute: Deutsches Zentrum für Neurodegenerative Erkrankungen (DZNE), Magdeburg

Graz & Magdeburg, December 2017

EIDESSTATTLICHE ERKLÄRUNG

Ich erkläre an Eidesstatt, dass ich die vorliegende Arbeit selbstständig verfasst, andere als die angegebenen Quellen/Hilfsmittel nicht benutzt, und die den benutzten Quellen wörtlich und inhaltlich entnommenen habe.

Graz, im Dezember 2017

(Unterschrift)

STATUTORY DECLARATION

I declare that I have authored this thesis independently, that I have not used other than the declared sources / resources, and that I have explicitly marked all material, which has been quoted either literally or by content from the used sources.

Graz, December 2017

(Signature)

ACKNOWLEDGEMENT

I would like to grasp this opportunity to show my greatest appreciation to all people who made this work possible. First and far most, I would like to express my deepest gratitude to Prof. Alexander Dityatev who opened widely the doors of his laboratory for me to explore and integrate the fascinating world of research. As well, I owe a debt of appreciation to my supervisors Maura Ferrer-Ferrer, Gabriela Matuszko and Dr. Rahul Kaushik for their patience, time and guidance. I also would like to thank all the Neuroplast team members and technical assistants for being greatly tolerant, supportive and inspiring.

I am very grateful to Assoc. Prof. Manfred Hartbauer for his endless aid, insightful and constructive comments and warm encouragement.

Special appreciation goes to my family who has been my source of strength and ambition. You are my all! Nothing would have been possible without you! I cannot forget to acknowledge people who provided a loving familial atmosphere and filled my stay with laughter and smiles, my friends, Vignesh, Hanady, Oliver, Carla, Antonia, Dr. Rajeev and my Karate classmates. You will always have a special place in my heart.

Definitely, I am very thankful to my classmates, for wonderful two years of scientific discussions and friendly conversations. I wish you all the success and happiness in days to come! Prost!

ABSTRACT

Studies of memory and learning at the molecular level revealed that neurotrypsin-mediated proteolysis of Agrin is indispensable for normal synaptogenesis and its impairment leads to recessive nonsyndromic mental retardation. This molecular mechanism influences dendritic filopodia formation and synaptogenesis. Previous research demonstrated that activity-dependent formation of dendritic filopodia is disrupted in hippocampus cultures obtained from neurotrypsin-knockout mice, but administration of the neurotrypsin-dependent 22-kDa fragment of Agrin rescued filopodial outgrowth. This Agrin fragment has strong influence on synapse formation, because dendritic filopodia are thought to be precursors of synapses.

The essential minimal fragment for Agrin signaling in the CNS is the 22-kDa COOH-terminal portion of this protein. The deletion of required sequences beyond the 20-kDa fragment yields a 15-kDa fragment that acts as an Agrin-22kDa antagonist that was found to suppress the induction caused by the 22-kDa fragment of Agrin (Hoover, Hilgenberg, & Smith, 2003). In this thesis, I aimed to provide evidence for the crucial role of the Agrin 22-kDa fragment on spinogenesis and synaptogenesis using overexpression adeno-associated viruses.

For this purpose, I cloned two expression vectors carrying the sequences for both the Agrin C-22kDa and C-15kDa fragment. Using these expression vectors, two overexpression adeno-associated viruses (AAV) were produced to express recombinant Agrin C-22kDa and C-15kDa proteins in ippocampus cells. I expressed these fragments in wild-type neurons as well as in neurortrypsin-deficient hippocampal cultures. I quantified the synaptic density of C-22kDa-related fluorescece by measuring the presynaptic, postsynaptic and co-localized puncta per dendritic area.

Using immunostainings and confocal microscope, I was able to demonstrate the synaptic accumulation of Agrin C-22kDa at synapses. In vitro assessment of the overexpressed C-22kDa Agrin accumulation at synapses in neurotrypsin-deficient cultures failed to reveal a significant effect on synaptic density in comparison to its antagonist (overexpressed C-15kD). This unexpected observation may be attributed to a low sample size and the bad condition of neurotrypsin-deficient hippocampal cultures. However, I was able to demonstrate AAV-driven expression of C-22kDa and its antagonist in this model system.

Table of Contents

1. INTRODUCTION

1.1 Memory and learning

The concepts of memory and learning are central for neuroscience. Learning is the process for acquiring memory. Episodic and semantic long-term memory leads to behavioral changes arising from experience. Neuroscientists divide long-term memory into two main categories: declarative (explicit) and implicit memory. Facts and past events from the declarative memory are divided into semantic (general world memory with a meaning) and episodic memory (time, places, associated emotions etc. That can be stated). In contrast, the non-declarative memory system includes skills, priming, classical conditioning, habituation and sensitization (Eysenck, 2012). The main difference between declarative (explicit) and non-declarative (implicit) memory arises from the fact that the first is consciously activated, whereas we are unaware of the latter type of memory. An example for implicit memory is the priming phenomenon, like remembering words to a song and finishing the line of the song when someone sings first two words. According to this distinction, between declarative and non-declarative memory, neuroscientists postulate different mechanisms for each type of memory and related processes are probably located in separate areas of the brain. For instance, the explicit memory is located in the neocortex, amygdala and hippocampus while implicit memory is found in the cerebellum and basal ganglia (Figure1)(Eichenbaum, H., & Cohen, 2001)

Figure 1 : Brain areas involved in memory (Eichenbaum, H., & Cohen, 2001).

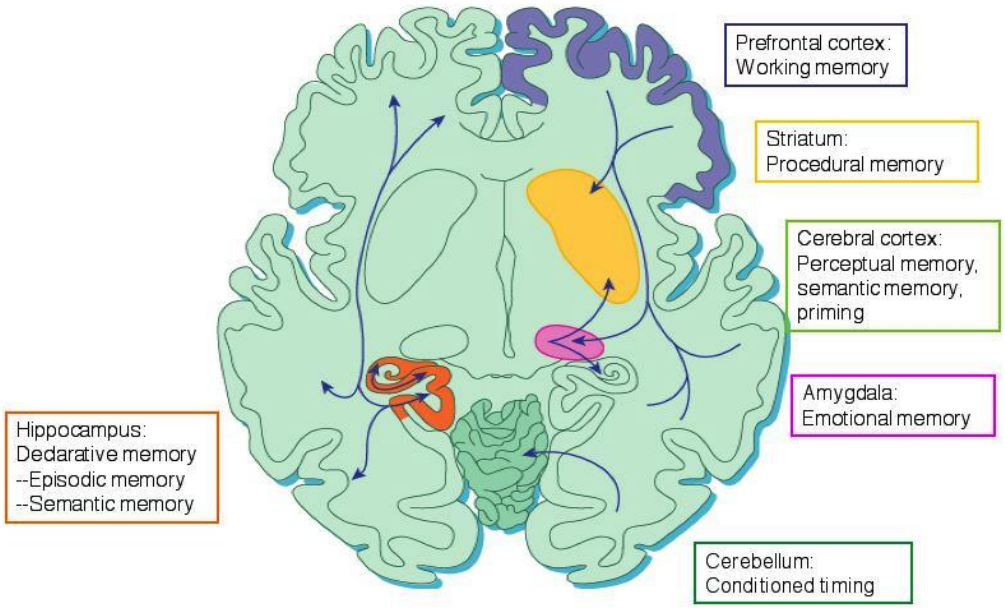

1.2 Memory Formation

The hippocampus is involved in the formation of different types of memory (Riedel & Micheau, 2001). The hippocampus consists of dentate gyrus (DG) and Cornu Ammonis (CA), which is an increasingly important area in hippocampal studies. It has been differentiated into distinct regions named CA1, CA2, CA3 and CA4. The CA3 region is of particular interest due to its specific role involving in memory processes (Cherubini & Miles, 2015). The entorhinal cortex (EC) and subiculum form other parts of the hippocampus in addition to DG and CA. The trisynaptic circuit is a fundamental pathway in hippocampus that was described by the neuroanatomist Santiago Ramon y Cajal. The entorhinal cortex projects via the preforant path (PP) onto mossy fibers of the granule cells of the dentate gyrus (DG). The CA3 region comprises a homogenous set of pyramidal cells, which receive inputs through synapses with mossy fibers of the DG. Pyramidal cells of CA3 project their axons via Schaffer collaterals onto *stratum radiatum* in CA1. CA1 is thought to decode memories to be sent back subsequently to the subiculum and deep layers of the entorhinal cortex for long-term storage (Figure2)(Florian & Roullet, 2004; Goda & Stevens, 1996; Izumi & Zorumski, 2008).
The Schaffer collaterals are important for plasticity in the hippocampus and plays a considerable role in many aspects of memory an learning (Squire, 2009).

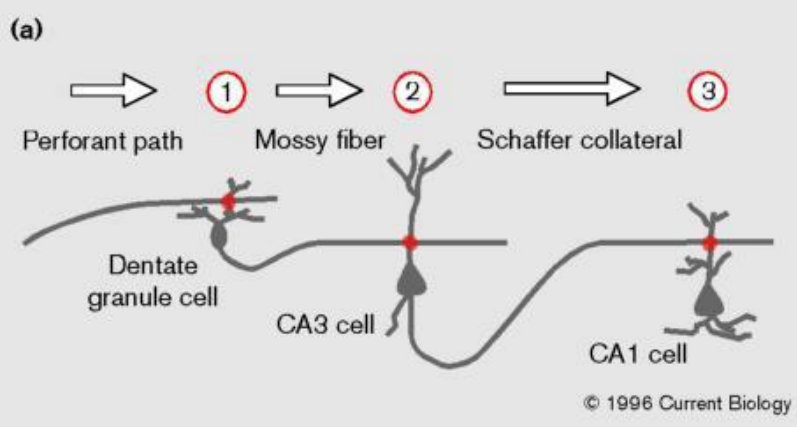

Figure 2: Schematic representation of the trisynaptic circuit in the hippocampus. The entorhinal cortex projects onto mossy fibers of the DG and the information is processed at the dendrites of CA3 pyramidal cells. Finally, infromation is transferred to the CA1 cells via Schaffer colaterals (Goda & Stevens, 1996).

1.3 Synaptic Plasticity

Central to memory and learning is the concept that regards the synapse as the pivotal site of memory formation. Distinct changes in communication among nerve cells signal transmission and related chains of events involved in synaptogenesis and synaptic plasticity has been considered important for memory and learning. Memory formation has a temporal domain and one can distinguish between short-term plasticity (STP) and long-term plasticity (LTP)(Okano, H., Hirano, T., & Balaban, E. (2000).;(Ohno et al., 2011)).

1.3.1 Short-term Synaptic Plasticity (STSP)

Short-Term synaptic plasticity is regarded as use-dependent presynaptic plasticity that occurs in timescales of milliseconds up to few minutes. Enhancement and depression are two forms of STP that either lead to the strengthening or weakening of the synaptic strength. STP are regulated by several factors whereby presynaptic calcium signaling, the vesicle pool and postsynaptic factors are the most prominent among them (Ben Achour & Pascual, 2010; Regehr, 2012).

1.3.2 Long-term Synaptic Plasticity (LTSP)

LTSP denotes memory formation that lasts minutes to few hours and occurs at excitatory synapses. Activity-dependent factors alter the synaptic strength through Long-term potentiation (LTP) and Long-term depression (LTD) (Yang & Calakos, 2013) (Lynch, 2004). The molecular mechanism of LTP involves NMDA-(N-methyl-D-aspartate) and AMPA-(amino-3-hydroxy-5-methyl-4-isoxazolepropionate) glutamate receptors, both are recruited after synaptic depolarization. A weak stimulation triggers the activation of AMPA receptors, while NMDA receptors remain inactive through Mg^{2+} blockage. When the postsynaptic marker is depolarized sufficiently, the postsynaptic responsiveness and excitability level is enhanced after the release of large amounts of glutamate from presynaptic terminals. This unblocks the NMDA receptor and leads to a Ca^{2+} influx, and bursts of action potentials (Figure 3)(Blundon & Zakharenko, 2008; Cleva, Gass, Widholm, & Olive, 2010).
At an early phase of LTP, Ca^{2+} activates the Ca^{2+}-calmodulin-dependent protein kinase II (CamKII) that phosphorylates AMPA receptors. CamKII and other activated protein kinases recruit more AMPA receptors into the postsynaptic membrane. This circuit is thought to be associated with short memory storage (Dityatev & Schachner, 2003; Malenka et al., 1989).
In a later phase of LTP, new proteins are synthesized and the cAMP-response element-binding protein (CREB) is activated to further enhance spinogenesis and synaptogenesis. This process is well-documented and leads to store long term memory formation (Dityatev & Schachner, 2003; Lakhina et al., 2015).

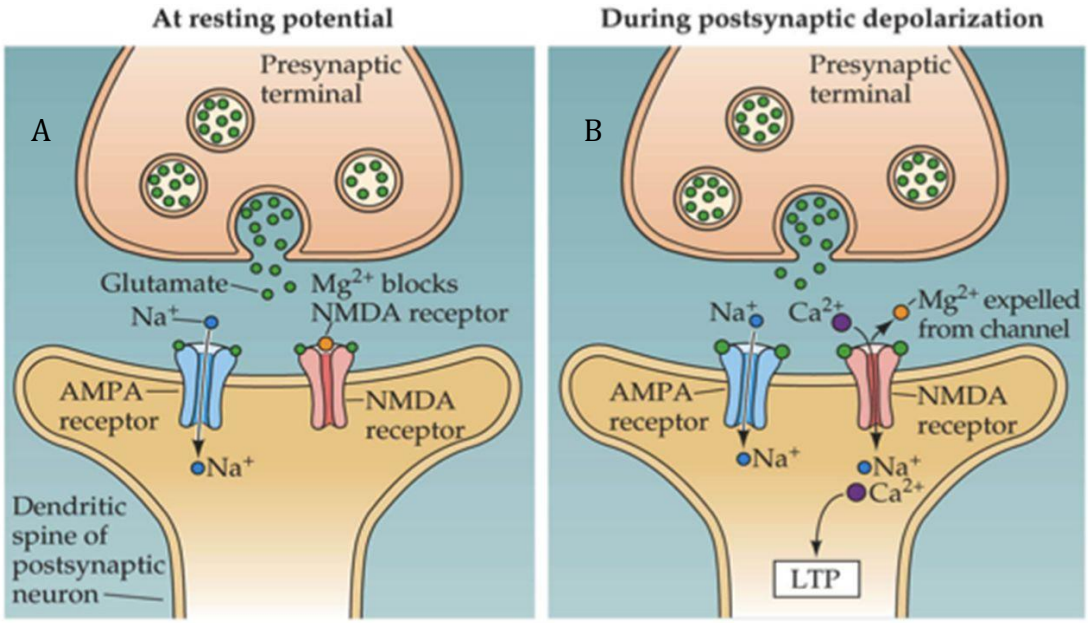

Figure 3: NMDA-receptor activation during depolarization. (A) At resting potential, the NMDR channel is blocked by Mg^{2+} but Na^{+} can pass the AMPA channel. (B) After membrane depolarization, Mg^{2+} is explled and and Ca^{2+} pass through the NMDA channel ("Neuroscience - Block IV Flashcards | Memorang," n.d.).

1.4 Extracellular Matrix (ECM)

This thesis is investigating the crucial role of an extracellular matrix molecule and the following gives an overview of the extracellular matrix and its molecules.

The extracellular space of the brain consists of a highly organized extracellular matrix (ECM). " ECM molecules are synthesized by neurons, glia and non-neural cells and are secreted into the extracellular space where they regulate synaptic plasticity " (Dityatev, Schachner, & Sonderegger, 2010). Recent research has shown that neuronal matrix modulations have an influence on synapses, morphologically and functionally. For example, it interferes with the induction or maintanence of long-term potentiation, which directly affects memory formation and, thus learning (Bonneh-Barkay & Wiley, 2009). The following describes ECM molecules and how they contribute to the structure and functions of synapses.

1.4.1 ECM Molecules and their importance in synaptic plasticity

Extracellular matrix molecules are accumulated in the form of a stable lattice-like network structure, known as the perineuronal net (PNNs) in the CNS (Wlodarczyk, Mukhina, Kaczmarek, & Dityatev, 2011). Synapses on the cell soma and proximal dendrites are embedded within the PNNs. The PNNs provides a solid surface in which ECM components (e.g. molecules, receptors and enzymes, etc) interact and exert influence on dendritic spines and synapses. These ECM molecules mainly include unbranched hyaluronic acid, chondroitin sulphate proteoglycans (CSPGs) and proteoglycans from the lectican family (e.g. aggrecan, versican, brevican, neurocan). In addition, there are various other proteoglycans and glycoproteins such as heparan sulphate proteoglycan (HSPGs), reelin, tenascins and laminins (Figure 4) (Khan, Muly, & Alkon, n.d.)

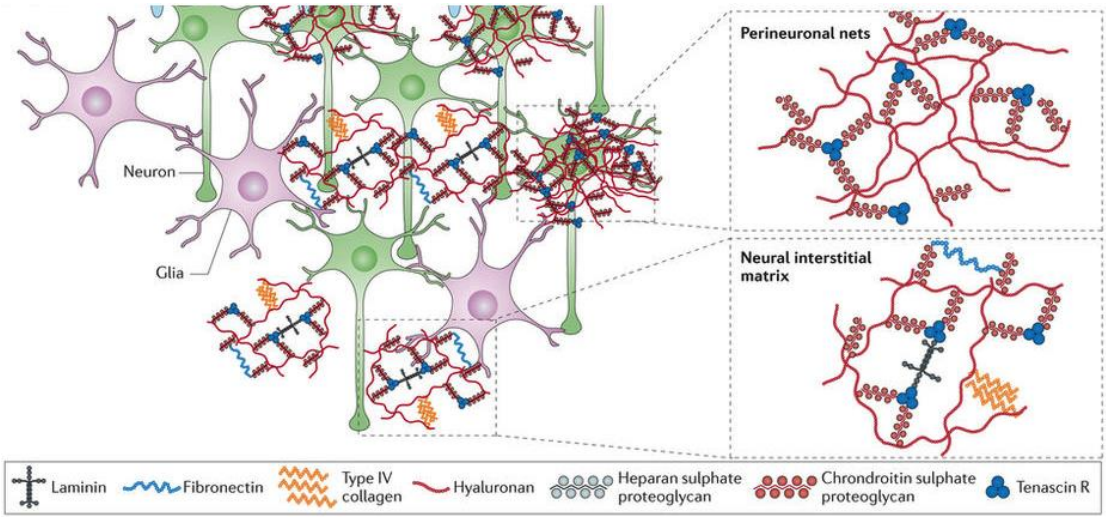

Figure 4: Structure of extracellular matrix (Lau, Cua, Keough, Haylock-Jacobs, & Yong, 2013).

Alteration of ECM composition causes abnormal dendritic spine development and synaptic plasticity, both leads to neurological disorders associated with memory loss, learning and other cognitive deficits (Khan et al., n.d.). The following section describes the results of a research focusing on effects of hyaluronic acid digestion.

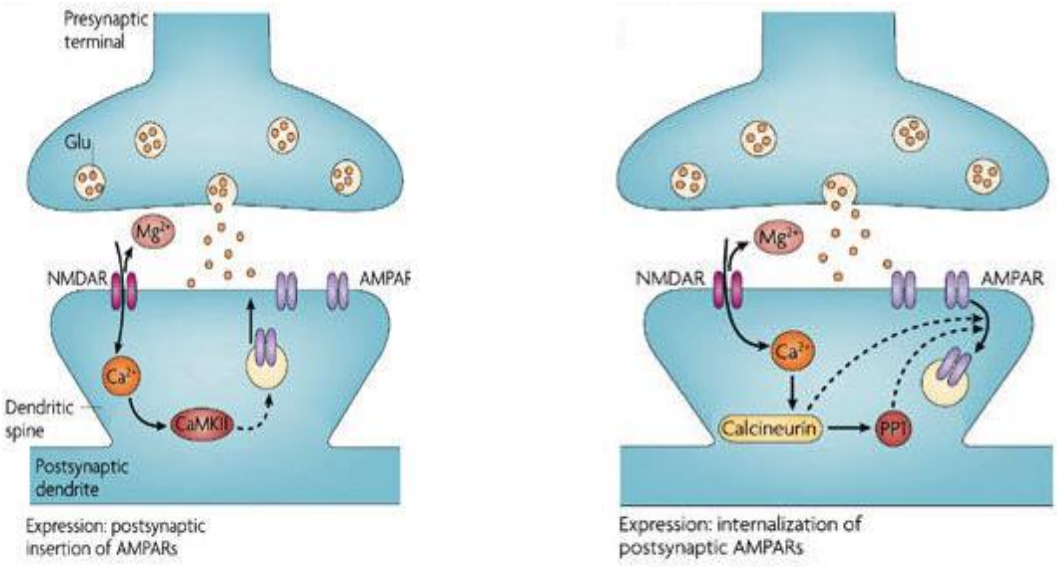

A B

Figure 5: NMDR-mediated LTP and LTD. After sufficient membrane depolarization, the NMDR channel is unblocked and Ca^{2+} interacts with either CamKII or Calcineurin, which activates signaling pathways.(A) This diagram represents NMDR-mediated LTP. CamKII-mediated signaling pathway leads to AMPARs exocytosis, which leads to LTP. (B) This diagram represents NMDR-mediated LTD. Calcineurin-mediated signaling pathway leads to AMPARs endocytosis which results in LTD (Kauer & Malenka, 2007).

Previous research has revealed that depletion of hyaluronic acid by hyaluronidase suppresses currents mediated by L-VDCCs. This suppression leads to the decrease of postsynaptic dendrite formation or spinogenesis and, thus abolishes the L-VDCC-mediated component of LTP. Administration of hyaluronic acid rescues the LTP effect of suppressed L-VDCCs. Therefore, extracellular matrix backbone, hyaluronic acid, plays a major role in synaptic plasticity (Wlodarczyk et al., 2011).

1.4.2 ECM receptors

Studies of ECM receptors and their ligands revealed their important role in neural communication, synaptogenesis and synaptic plasticity. Once a synapse is established, ECM receptors maintain neural connection and regulate the plasticity of synapses. Ligand-bound ECM receptors activate downstream signaling cascades that control cytoskeletal dynamics and synapse plasticity and thereby influence cell fate, memory and learning (Dityatev, Wehrle-Haller, & Pitkänen). The major ECM receptors are integrin, syndecan, lipoprotein and Agrin receptors.

1.4.2.1 Integrin

Integrin-R is adhesion receptor and consists of a heterodimer αβ-subunit. Studies over the past two decades have revealed important information on integrin α subunits in synaptic plasticity and LTP (Dityatev et al., 2010). Moreover, the cytoplasmic tail of the Integrin β subunit can activate kinase signaling cascades and affect spinogenesis. In particular, α3, α5, α8, α (V), β1, and β3 have an important role in the brain for neural communication, synapse and dendrite development, maturation, stabilization and synaptic plasticity. Characterization of integrins in hippocampal neurons showed that α5 β1 integrins are localized in the dendritic spines where they regulate spinogenesis and synaptogenesis. This localization is activity-dependent, whereby glutamate stimulation enhances the concentration of integrin in dendritic spines. Due to this dominant role of integrin-R, any disruption or deficit of it impairs behavioral tasks, particularly, learning and memory (Dityatev et al., n.d.; Harburger & Calderwood, 2009).

1.4.2.2 Syndecan

Syndecan is one of the transmembrane HSPGs class consisting of four members, syndecan 1-4. Syndecan-2-3 are predominantly expressed in the brain (Carey, 1997), where their indispensable role in neuronal development, dendritic spinogenesis and synaptic plasticity have been described (Ethell & Yamaguchi, 1999). Despite little is known about underlying mechanisms, activation of syndecans 2-3 mediate downstream signaling cascade, which ultimately impacts cognitive functions like memory and learning (Ethell & Yamaguchi, 1999; 2002).

1.4.2.3 Lipoprotein receptors

In CNS, cholesterol homeostasis regulates synaptic plasticity (Koudinov & Koudinova, 2001). Due to the fact that cholesterol neither enters nor exits the blood-brain barrier (BBB) (Lin et al., 2016) in situ biosynthesis of cholesterol is the only way to supply brain with cholesterol. Cholesterol synthesis is mediated by both non-neuronal and neuronal cells, the latter in smaller quantities.

24S-hydroxycholesterol is a cholesterol-derived metabolite that penetrates the BBB. To maintain synaptic plasticity, CNS lipoprotein redistribute cholesterol to non-neuronal and neuronal cells, following membrane repair and remodeling, biogenesis of organelle and synapse formation (Mahley, 2016).

1.4.2.4 Agrin

In addition to other ECM molecules, Agrin plays a crucial role for synaptogenesis, synaptic plasticity, thus LTP and memory formation. Data from several studies suggest Agrin as a modulator of spinogenesis and synaptogenesis (McCroskery, Bailey, Lin, & Daniels, 2009). This master thesis aims to contribute

to this growing area of research by elucidating the key role of Agrin in synaptic plasticity, which represents the basic mechanism underlying memory and learning.
Agrin has long been known from the neuromascular junction (NMJ) where it is important for the clustering of acetylcholine receptors (MuSK) on the skeletal muscle cell (Rupp, Payan, Magill-Solc, Cowan, & Scheller, 1991). At the NMJ, Agrin is found in a secreted form in the basal lamina of the skeletal muscle cell (Reist, Magill, & McMahan, 1987), whereas the transmembrane form of Agrin has been found in the brain (Ramseger, White, & Kröger, 2009). Splice sites present in the N-terminus of Agrin give rise to secreted and trans-membrane forms. In addition, there are A/y and B/z splice sites in the C-terminal, where it enables heparin binding and AChR clustering, respectively (Figure 6) (Singhal & Martin, 2011).

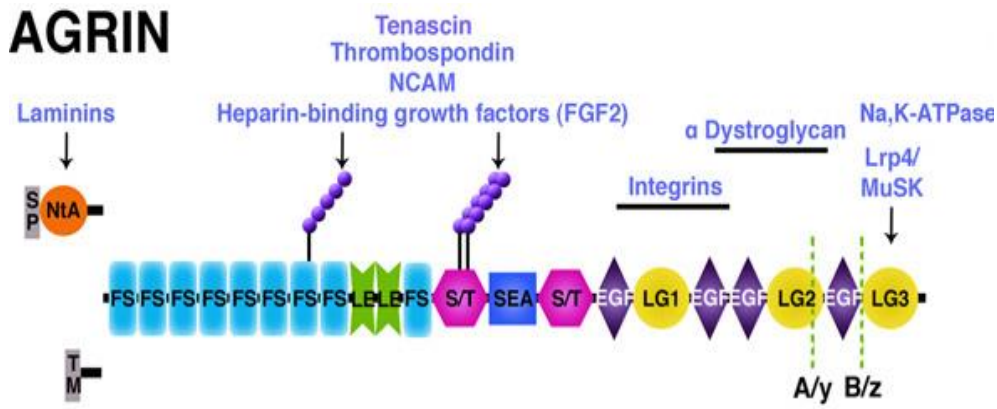

Figure 6: Molecular structure of Agrin. Legend: NtA, N-terminal Agrin-laminine binding; SP, Signal peptide; TM, Transmembrane domain; FS, Follistatin-like domain; LB, Laminine B domain; S/T, Serine/threonine-rich murin-like domain; SEA, Sea urchin sperm, enterokinase and Agrin domain; EGF, Epidermal growth factor-like repeat; LG, Laminin-like globular domain; Lrp4, Low-density lipoprotein receptor-related protein4; MuSK, Muscle-specific kinase; A/y and B/z splice sits in C-terminal (Singhal & Martin, 2011).

1.5 Agrin knock-out mouse models

Experiments performed with Agrin-null mice did not support the role of Agrin in synaptogenesis (Daniels, 2012) in the brain. However, studies demonstrated a notable reduction of synaptogenesis in hippocampal cell cultures where Agrin expression was suppressed by the addition of antisense oligonucleotides, or by the introduction of lentiviral vector expressing Agrin small-interfering RNA. Hence, this study did not support the previously published studies on the effcet of Agrin on synaptogenesis. However, administration of Agrin to the above mentioned cultures mediated activation of signaling pathways that are thought to regulate the synapse function, including, transcription factor CREB,

immediate-early gene c-fos, or the mitogen-activated protein (MAP) kinase pathway (Ksiazek et al., 2007). The inconsistency between *in vivo* and *in vitro* studies suggest that syndecan may rescue the chronic absence of Agrin in Agrin-null mice (Daniels, 2012).
Further research examined the effect of Agrin on synaptic density by means of transgenic mouse models that did not express endogenous Agrin but chicken secretory Agrin. Although secretory Agrin at the NMJ improved mice development, histology revealed a 30% reduction of excitatory synapses of cortical neurons, diminished dendritic spine density and scaled-down excitatory postsynaptic potentials (Bose et al., 2000). In summary, Agrin triggers sets of neuron-specific gene transcriptions, which induces the elongation and branching of neurites in the CNS (Mantych & Ferreira, 2001).

1.6 Extracellular proteolysis and synaptic plasticity

Extracellular proteolysis is crucial for synaptic plasticity and mechanisms underlying cognitive functions (Frischknecht, Fejtova, Viesti, Stephan, & Sonderegger, 2008). Previous research emphasized the critical role of neurotrypsin-mediated proteolysis for normal synapse function. It has been observed that mutated neuronal serine protease neurotrypsin gene was linked with autosomal recessive nonsyndromic mental retardation. In addition, it has been shown that neurotrypsin expression is high in brain areas involved in memory and learning (Molinari et al., 2002).
Several studies have shown that neurotrypsin is accumulated at the presynaptic boutons, where short depolarization triggers neurotrypsin exocytosis. In addition, neurotrypsin is released activity-dependently and mediates proteolytic Agrin cleavage at the synaptic cleft (Matsumoto-Miyai et al., 2009; Molinari et al., 2002). However, research has consistently shown that neurotrypsin exocytosis depended on the presynaptic depolarization and P/Q/N-type calcium channel activation. Additionally, neurotrypsin is released in an inactive form and postsynaptic NMDR-Rs activation is indispensable for neurotrypsin activation leading to Agrin cleavage (Matsumoto-Miyai et al., 2009).
As mentioned in section 1.3.2, LTP depends on to the significant rise of the postsynaptic [ca^{2+}], its influence on signaling cascades, and the recruitment of respective receptors (Nicoll & Malenka, 1999). Therefore, strong neuronal activity enhances neurotrypsin-dependent cleavage of Agrin at excitatory synapses (Matsumoto-Miyai et al., 2009).

In a recent study, researchers aimed to assess the effect of proteolytic Agrin cleavage (released C-Agrin22kDa) on isolated hippocampi and hippocampal slices, and indicated LTP dependent induction of dendritic filopodia. Filopodia are thought to be precursors of spinogensesis and synaptogenesis, together, these findings approve the crucial role of neurotrypsin and C-Agrin22kDa in *de novo* synapse formation as well as synaptic plasticity (Figure 7) (Daniels, 2012; Matsumoto-Miyai et al., 2009)

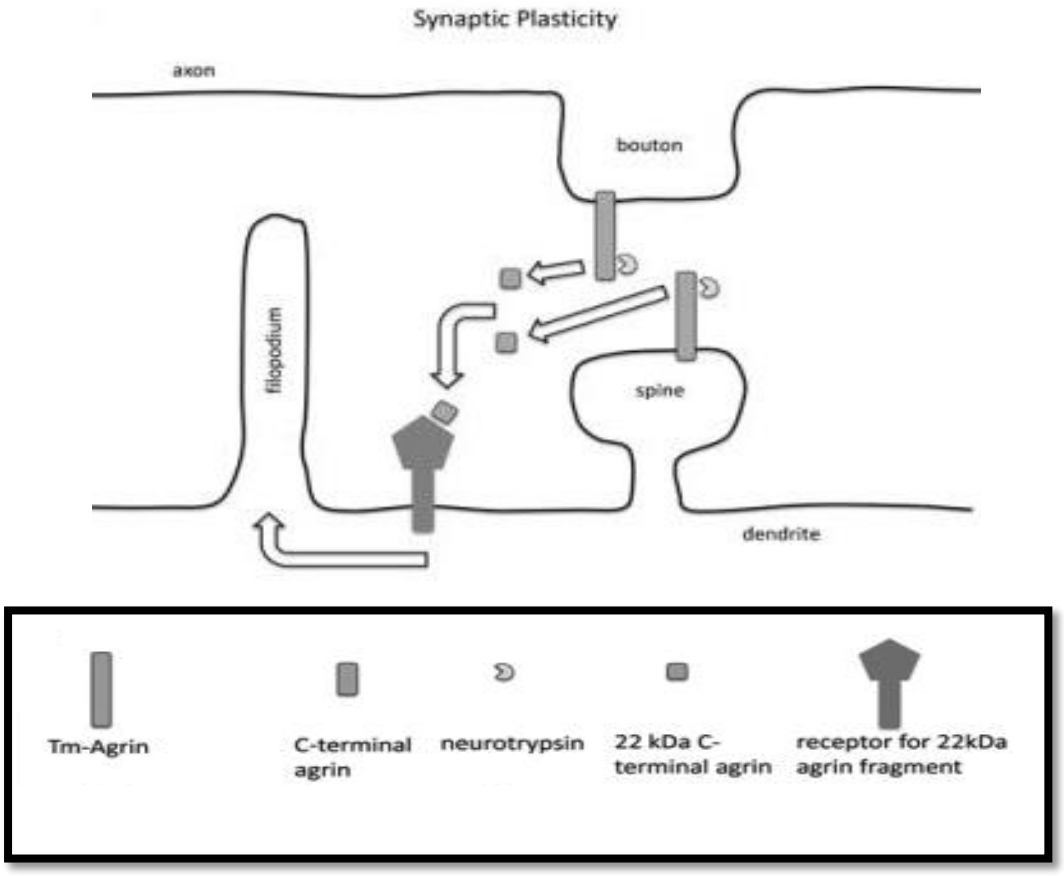

Figure 7: Postulated scheme of Agrin induced synapse formation. Under potentiated conditions (LTP), secreted neurotrypsin triggers Agrin cleavage which leads to the 22kDa C-terminal fragment(Matsumoto-Miyai et al., 2009). This fragment interacts with its receptor and induces filopodia development, considered as a precursor of synapses (Daniels, 2012)

Furthermore, the description of Agrin cleavage in hippocampal neurons of neurotrypsin-deficient mice has confirmed the eradication of dendritic filopodia formation (Matsumoto-Miyai et al., 2009).
There is an increasing research attempt to rescue this abolished filopodial response via supplying the target protein implicating filopodia development. Therefore, the following sections review some of the previously published results.

1.7 The role of Agrin C-terminal

The proteolytic substrate of neurotrypsin (Agrin) cleaves at two homologues α and β sites, lopping off a middle 90kDa and a C-terminal 22kDa fragment, respectively (Figure 8) (Stephan et al., 2008).
The characterization of these fragments was performed in pyramidal CA1 cells of hippocampal slices obtained from 4-6 weeks-old mice. Interestingly, adminstration of Agrin-22kDa relieved the filopodia-promoting abolishment in

neurotrypsin-knock out mice, whereas Agrin-90kD lacked this ability (Matsumoto-Miyai et al., 2009).

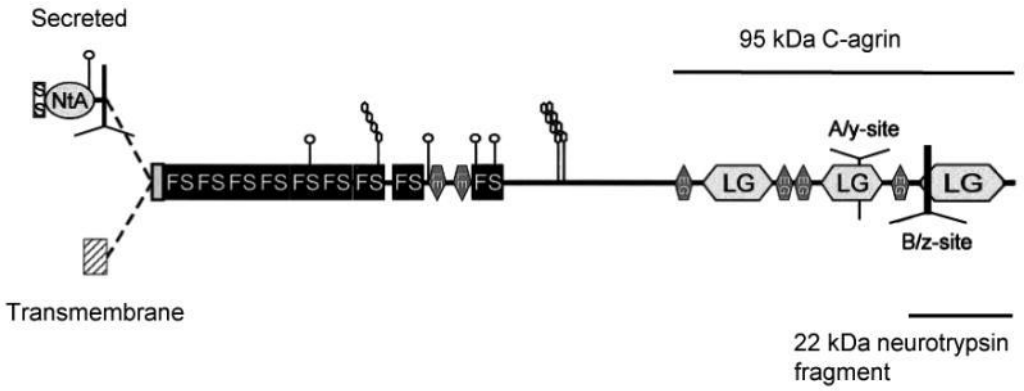

Figure 8: Scheme of Agrin structure. Modified from figure 1A (Neumann et al.,2001.)(Daniels, 2012).

1.8 C-Agrin15 kDa acts as competitive antagonist

Qualitative and quantitative research designs were developed to assess the effect of a smaller fragment of Agrin-22kDa and Agrin15-kDa. Despite the significant impact of Agrin-22kDa and Ag-90kDa on the resting intracellular Na^+ level of resting neurons, Agrin-15kDa showed no other stimulating effect. In contrast, Agrin15 had an inhibitory effect on membrane depolarization as well as on the activation of signaling cascades mediated through Agrin22kDa. Taken together, it seems that Agrin-15kDa antagonizes the induction mediated by Agrin22kDa (Hilgenberg, Su, Gu, O 'dowd, & Smith, n.d.).

1.9 MuSK, putative Agrin receptor in the brain

In addition to the role of MuSK at the neurromuscular junction, previous studies revealed that MuSK mRNA and the resulting protein are extensively expressed in the cortex, cerebellum and hippocampus of rat brain. In addition, some of these proteins turned up to be enriched at the excitatory synapse, where Agrin is abundant suggesting that probably MuSK co-localizes with Agrin at excitatory synapses (Figure 9) (Garcia-Osta et al., 2006; Ksiazek et al., 2007; Stephan et al., 2008).

Garcia-Osta and colleagues (2006) demonstrated that hippocampal MuSK expression is crucial for memory consolidation. Data from this research revealed that introducing MuSK antisense oligonucleotide inhibits MuSK expression, which impaired synaptic plasticity underlying memory consolidation and learning. MuSK inhibition hinders signal transduction pathways by restraining the phosphorylation of the transcription factor CREB as well as the

expression of the transcription factor CCAAT enhancer binding protein β (C/EBPβ) (Kandel, 2001).

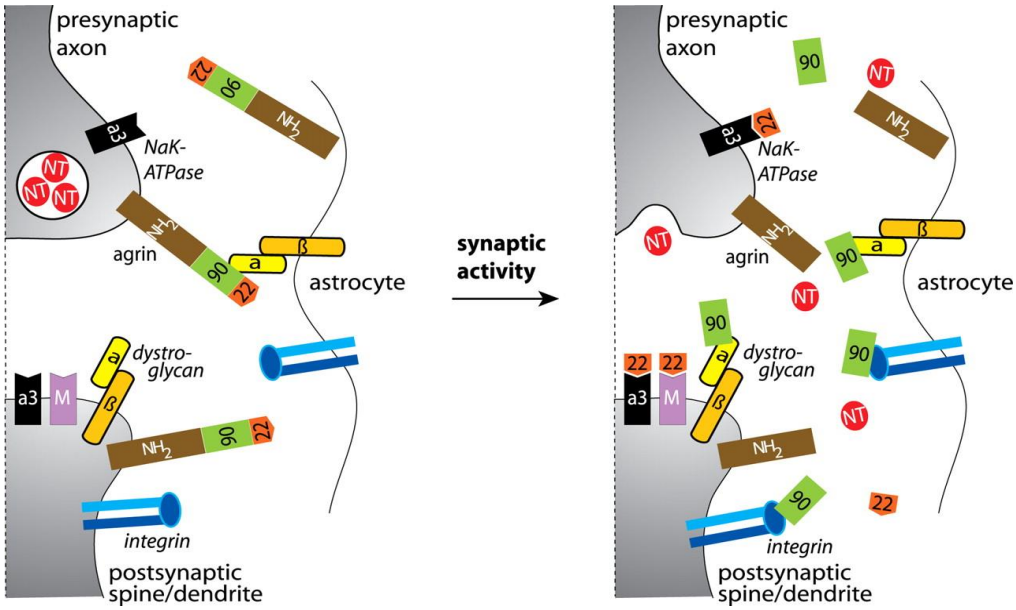

Figure 9: Model of neurotrypsin-dependent cleavage of Agrin CNS (Stephan et al., 2008). The cleaved 90kDa fragment of Agrin was shown to bind to integrins, α-dystroglycan, heparan sulfates enclosed in synapses (Clegg, Wingerd, Hikita, & Tolhurst, 2003; Yamaguchi, 2002). In addition, the C-22kDa fragment interacts with α3Na^+/K^+-ATPase and tyrosine kinase MuSK receptors. Recent studies have shown that MuSK receptors are present in CNS as well (Ksiazek et al., 2007). However, the details of Agrin-MuSK localization CNS are still unclear (Stephan et al., 2008).

1.10 The neuronal receptor for Agrin

Recent studies discovered that Agrin regulates the function of Na^+/K^+-ATPase, proposing a molecular model of Agrin-NKA (Na^+/k^+ ATPase, which precisely mediates the binding of C-Agrin22 to α3 subunit of NKA (Figure 9 and10) (Hilgenberg et al., n.d.). A low concentration of the C-Agrin22 fragment induces the intracellular Ca^{2+}-oscillations that leads to the activation of several signaling pathways associated with NF-κB (nuclear factor kappa-light-chain-enhancer of activated B cells), cell division and cell survival (Li, Zelenin, Aperia, & Aizman, 2006).
A high concentration of C-Agrin22 cause an elevation of intracellular sodium concentration. A high cytoplasmic concentration of sodium disrupts the function of Na/K pump, due to the potassium application (Tidow, Aperia, & Nissen, 2010). In the resting state, sodium/calcium exchanger (NCX) tends to pump Ca^{2+} out of the cell in order to maintain Ca^{2+} homeostasis. Whilst, NCX is pumping Na^+ in, maintaining the Na^+ electrochemical gradient that is indispensable for the generation of action potentials. The inhibited NKA reverses or slows the NCX operation (Tidow et al., 2010; Lisé & El-Husseini, 2006).. Moreover, membrane depolarization leads to the opening of Voltage-

gated calcium channels (VGCC) enabling Ca^{2+} influx (Hilgenberg, Su, Gu, O'Dowd, & Smith, 2006), and the reverse action of NCX rises the local Ca^{2+} concentration. This mechanism is important for the synaptic plasticity because a significant level of intracellular Ca^{2+} concentration is essential for the mechanisms underlying LTP and LTD (Tidow et al., 2010). Additionally, strong evidence was provided that C-Agrin22 increased the tyrosin phosphorylation of the α3 subunit of NAK pump, whereas C-Agrin15 decreased. The presence of C-Agrin15 competed to block the generation of action potentials by impairing native Agrin- α3Na^+/K^+-ATPase interaction (Hilgenberg et al., n.d.).

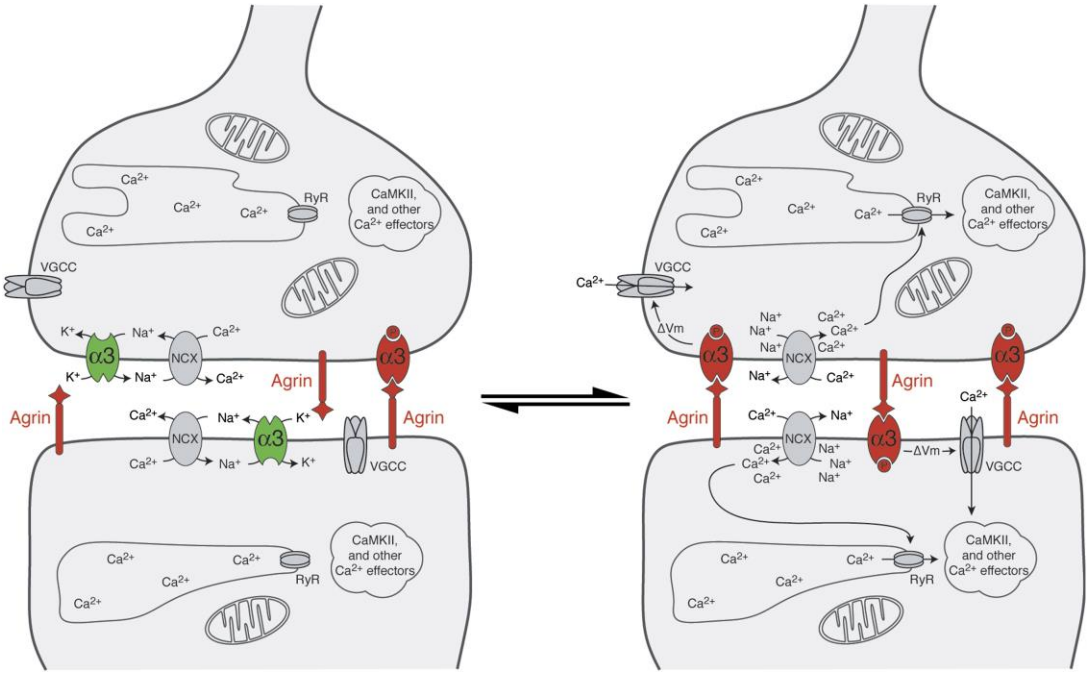

Figure 10: Model of Agrin- α3Na^+/K^+-ATPase interaction at the synapse. (Left) In the resting state, sodium/calcium exchanger (NCX) tends to pump Ca^{2+} out of the cell in order to maintain Ca^{2+} homeostasis while pumping Na^+ in, (Right) When Agrin- α 3Na^+/K^+-ATPase is formed, is leading to the high concentration of Sodium. An elevation of cytoplasmic concentration of Na^+ inhibits the function of the Na^+/K^+-ATPase pump. The inhibited NKA reverses or slows the NCX operation, this reverse action rises intracellular concentration of Ca^{2+} and diminishes the intracellular concentration of Na^+.

.

2. OBJECTIVE

To date, the understanding of how the synapse contributes to mechanisms underlying learning and memory is a prominent topic in neuroscience. In this context, synaptic plasticity plays a key roleand forms the basis of Long-term Potentiation and Long-term Depression, which are regulated by vaious factors and/or components. Research in the last two decades has focused on the elucidation of the role of Agrin in the brain that is an extracellular matrix protein. This effort revealed its crucial role for the neuromuscular junction as well as in the central nervous system.

In my thesis I studied the functional role of C-Agrin22kDa by measuring the density of excitatory synapses in wild type and neurotrypsin-knockout hippocampal cell cultures, by means of an adeno-associated virus that leads to overexpression of C-Agrin22kDa. According to the mentioned theories mentioned in the introduction of this thesis, neurotrypsin and Agrin are both essential for synaptogenesis. In the absence of neurotrypsin the proteolytic cleavage of Agrin does not occur and filopodial response is abolished. To design a rescue experiment, the neurotrypsin-knock out cultures were prepared and infected by overexpression adeno-associated viruse C-Ag-22kDa.
In a control group, I used the antagonist of this fragment, namely C-Agrin-15kDa. For this purpose, two expression vectors expressing either C-Agrin22kDa or its antagonist (C-Agrin15kDa) had to be cloned for virus preparation. Moreover, we assessed the in vitro validation of these viruses in wild type and knockout cultures to examine the effect of C-Agrin22kDa and its antagonist (C-Agrin15kDa) on synaptic density.
After virus infection, I expected the wild-type culture to have a higher synaptic density and the neurotrypsin-knock out culture to be rescued.

3. METHODS AND MATERIALS

3.1 Basic experimental set-up

To produce the overexpression adeno-associated viruses, the EST (Expressed sequence tag) partially sequenced mouse Agrin cDNA (Table 1) had to be cloned into expression vectors.

Workflow of the overexpression Adeno-associated viruse (AAV)

1. Cloning Agrin insert into pAAV vector backbone
2. Identifying the respective clone carrying the gene of interest
3. Transfecting HEK293T cells
4. Virus titration

Further, these viruses were used to infect the wild type as well as the neurotrypsin-knockout cultures and their expression was studied by means of immune staining.

3.1.1 PLASMIDS AND VIRUSES

3.1.1.1 Initial plasmids and primers

The initial plasmids and primers used in this thesis are listed in table 1 and 2. The initial vectors and primers for construction of the plasmids in this thesis were kindly provided by Dr.Rahul Kaushik. The initial plasmid was contained Synapsin 1 gene, which confers vastly neuron-specific long-term transgene expression from an adenoviral vector. It should be noted that this plasmid was previously tagged with mScarlet. The mScarlet is an bright monomeric red flourescent protein.

Table 1 : Initial plasmids.

Name of initial plasmid	Produced by	Resistance Marker
pAAV-Synapsin1-CPTX_Ruby2_WPRE_Sv40	Dr.Rahul kaushik & Gabriela Matuszko	Amp
pAAV_Syn1_Kozak_mHAPLN1_mScarlet_WPRE	Dr.Rahul Kaushik	Amp
EST Partially sequenced mouse Agrin cDNA		Kan

*The resistance marker is an antibiotic resistance gene.

Table 2 : Primers used in this thesis.

Intr. No.	Oligonucleoties	Sequence
315	pAAV_Syn_Agrin-22_Scarlet_WPRE_EcoR1_Fw	5'-TAAGCAGAATTCGCCACCATGTCAGTGGGGGACCTAGAAACAC-3'
316	pAAV_Syn_Agrin-22/Agrin-15_Scarlet_WPRE_Xho1_Rev	5'-TAAGCACTCGAGGAGAGTGGGGCAGGGTCTTAG-3'
317	pAAV_Syn_Agrin-15_Scarlet_WPRE_EcoR1_Fw	5'-TAAGCAGAATTCGCCACCATGTGGATTGGAAAGGTTGGAGAACG-3'
318	pAAV_Syn_Sec(CPTX)_Agrin-22_Scarlet_WPRE_Age1_Fw	5'-TAAGCAACCGGTTCAGTGGGGGACCTAGAAACAC-3'
319	pAAV_Syn_Sec(CPTX)_Agrin-22 and Agrin-15_Scarlet_WPRE_Xba1_Rev	5'-TAAGCATCTAGACATATGGTCGACGAGCTCG-3'
320	pAAV_Syn_Sec(CPTX)_Agrin-15_Scarlet_WPRE_Age1_Fw	5'-TAAGCAACCGGTTGGATTGGAAAGGTTGGAGAACG-3'

3.1.1.2 Two-step cloning and plasmids

Table 3 : List of generated plasmids.

No.	Plasmid Name	Resistance Marker
1	pAAV_Synapsin_Agrin22_Scarlet	Amp
2	pAAV_Synapsin_Agrin15_Scarlet	Amp
3	pAAV_Synapsin_SecretionSequence(CPTX)_Agrin22_Scarlet	Amp
4	pAAV_Synapsin_SecretionSequence(CPTX)_Agrin15_Scarlet	Amp

3.1.2.2.1 Construction of AAV_Synapsin_Agrin22_Scarlet and AAV_Synapsin_Agrin15_Scarlet

For this purpose, the initial vector AAV_Syn1_Kozak_mHAPLN1_mScarlet _WPRE (Table 1) was cut with XhoI and EcoRI to remove a fragment of 1074bp and the resulting 5526bp digested backbone was further processed to clone the gene of interest, namely the EST (Expressed sequence tag) partially sequenced mouse Agrin cDNA. The primers 315 and 316 (Table 2) were used for PCR amplification of the gene of interest (expected PCR product having 560bp) for the construction of AAV_Synapsin_Agrin22_Scarlet (Figure 11). The primers 316 and 317 (Table 2) were used for PCR amplification of the gene of interest (expected PCR product having 420bp) for construction of AAV_Synapsin_Agrin15_Scarlet (Figure 12). The ligation reaction mixes were transformed into NEB® Stable Competent *E. Coli* and plated on LB-Amp plates. Finally, the vector 1 and 2 (Table 3) were sequenced and sequencing results identified the constructs that carry the genes of interest.

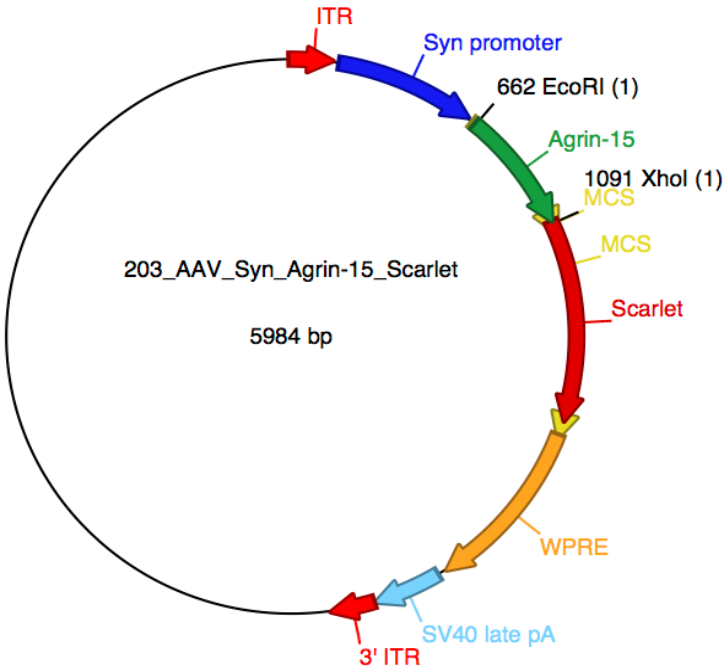

Figure 13: Vector map of AAV_Synapsin_Agrin22_Scarlet contained ITR-3', ITR-5', synapsin promoter, Gene of interest (Agrin22), Multiple cloning sites consist of our chosen restriction sites, Scarlet as reporter gene and the SV40 late polyA terminator. For the amplification of the virus concentration the woodchuck hepatitis virus posttranscriptional regulatory element (WPRE) was included.

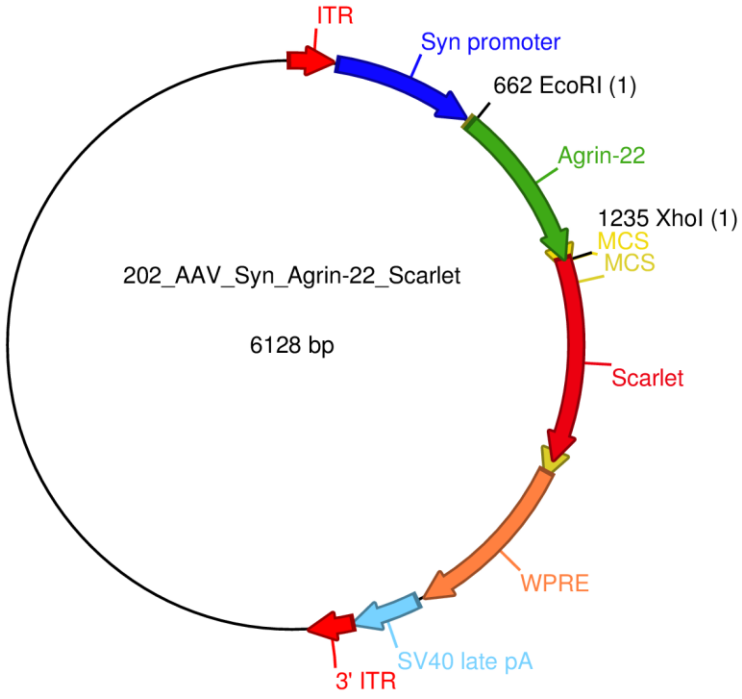

Figure 14: Vector map of AAV_Synapsin_Agrin15_Scarlet comprises the same vector elements as AAV_Synapsin_Agrin22_Scarlet (Figure 13) with one exception: the gene of interest Agrin22 was replaced by Agrin15.

3.1.2.2.2 Construction of AAV_Synapsin_SecretionSequence(CPTX) _Agrin22_Scarlet and AAV_Synapsin_SecretionSequence(CPTX)_ Agrin15_Scarlet

The recombinant vectors 1 and 2 (Table 3) from the cloning (see section 3.1.1.3) were used as PCR templates for the cloning of AAV_Synapsin_SecretionSequence(CPTX)_Agrin22_Scarlet and AAV_Synapsin_SecretionSequence(CPTX)_Agrin15_Scarlet.
AAV-Synapsin1-CPTX_Ruby2_WPRE_Sv40 was cut with AgeI and XbaI to eliminate two fragments (1443bps and 228bps). The resulting digested backbone was further used to clone the generated plasmids 1 and 2 (Table 3). Primers 318 and 319 (Table 2) were used for PCR amplification of the gene of interest (expected PCR product of 1287bps) for the construction of AAV_Synapsin_SecretionSequence(CPTX)_Agrin22_Scarlet (Figure 13) and primers 319 and 320 (Table 2) were used for PCR amplification of the gene of interest (expected PCR product of 1143bps) for the construction of AAV_Synapsin_SecretionSequence(CPTX)_Agrin15_Scarlet (Figure 14). The ligation reaction mixes were transformed into NEB® Stable Competent *E. Coli* and plated on LB-Amp plates.
Finally, the generated vectors 3 and 4 (Table 3) were sequenced and sequencing results identified the constructs to carry the genes of interest.

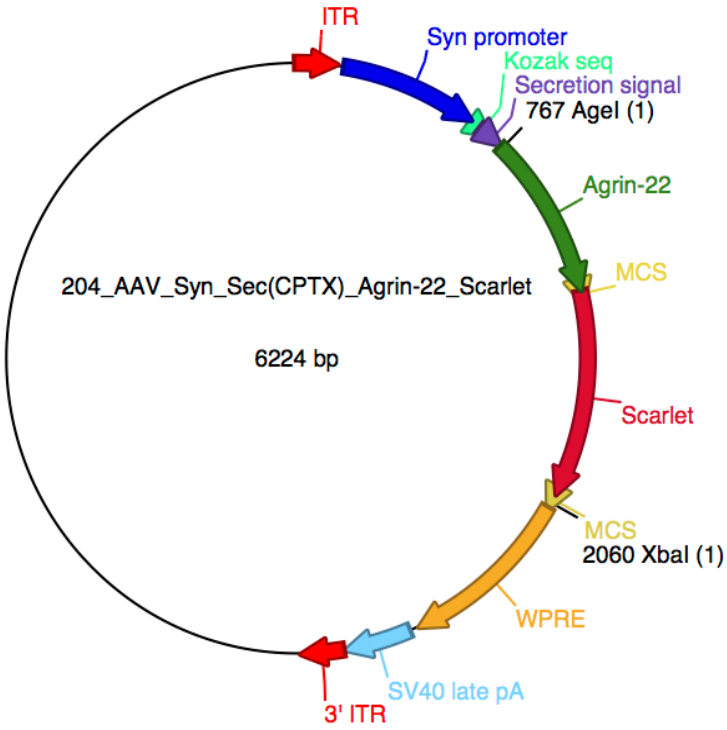

Figure 15: Vector map of AAV_Synapsin_SecretionSequence(CPTX)_Agrin22_Scarlet consisted of same vector elements as AAV_Synapsin_Agrin22_Scarlet (Figure 13) with two additional features:

Kozak sequence to be recognized by ribosome for further translational processes and secretion signal which helps the synthesized protein to be destined towards secretory pathway.

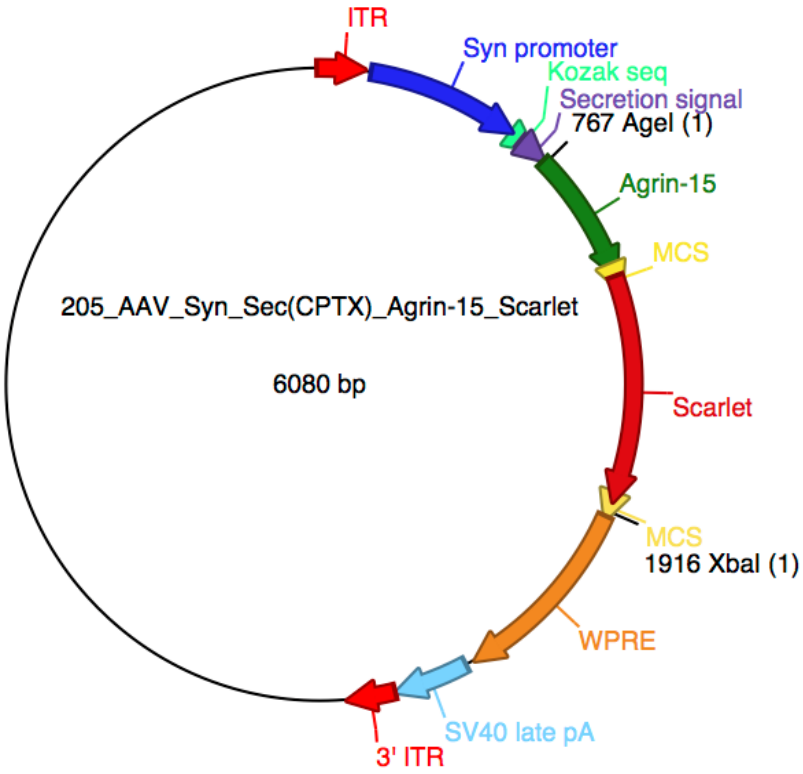

Figure 16: Vector map of AAV_Synapsin_SecretionSequence(CPTX)_Agrin15_Scarlet consisted of same vector elements as AAV_Synapsin_SecretionSequence(CPTX)_Agrin22_Scarlet (Figure 15), with an exception: the gene of interest (Agrin22) was replaced with Agrin15.

3.1.2 Viruses

Adeno-associated viruses AAV_Synapsin_ SecretionSequence (CPTX)_Agrin22_Scarlet and AAV_Synapsin_SecretionSequence (CPTX)_Agrin15_Scarlet were cloned in the course of this thesis. The viruses were prepared by transfecting HEK293 cells with a mixture of three plasmids pAAV-DJ (7.3Kb), pHelper (11.4Kb) and an expression vector with the molar ratio of 1:1:1. Expression plasmids 3 and 4 (Table 3) were transfected independently in order to produce two different AAV viruses.

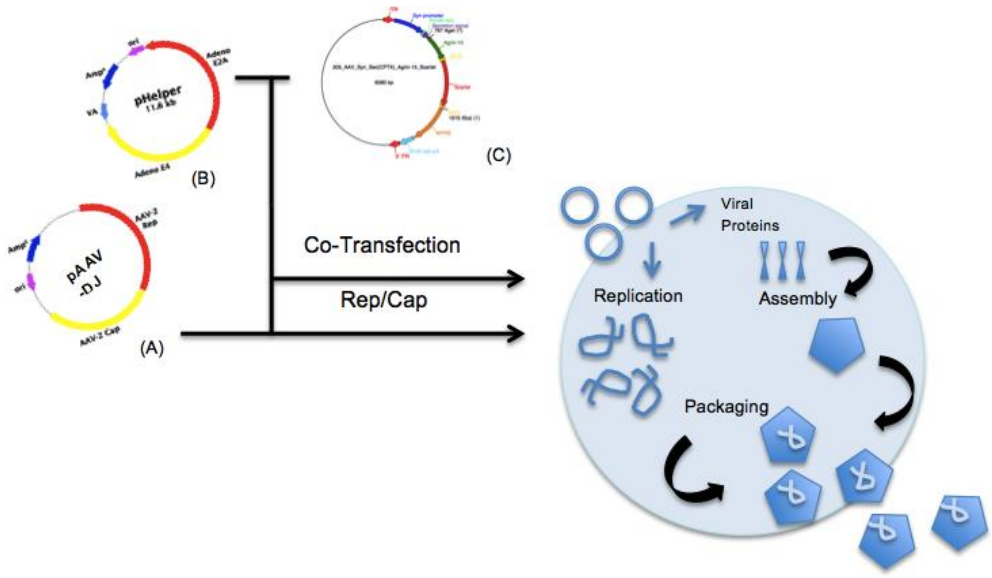

Figure 11: Schematic representation of AAV production in HEK293 cells. Adeno-associated viruses are obtained by transfecting HEK293 cells with three plasmids. (A) pAAV-DJ,comprises ITRs,Rep genes to produce Rep40,Rep52,Rep68,Rep78 that are indispensable for AAV-lifecycle the transfer plasmid and the Cap gene to produce viral proteins VP1,VP2,VP3-capsid proteins,(B) pHelper, supplies AAV genes (E4,E2a and VA) to transfer plasmid which mediates AAV replication, and (C) the expression vector. The transgene present in the expression plasmid integrates between the loci ITRs of pAAV-DJ. The replicated transgenes are assembled into the capsid and the viral particles are packaged.

3.2 KITS AND PROTOCOLS

3.2.1 Kits

3.2.1.1 Sigma Plasmid Maxipreps kit

The GenElute HP Plasmid DNA Maxiprep kit from Sigma-Aldrich Chemie GmbH (Germany) was used for the isolation of purified plasmid DNA in a large scale as described in the manufacturer instruction.

3.2.1.2 Macherey-Nägel PCR Clean-UP Gel extraction

The PCR Clean-UP Gel extraction from Macherey-Nägel GmbH & Co.KG (Berlin, Germany) was used to purify DNA after PCRs and digestion reactions Loading on gels was performed according to the manufacturer protocol.

3.2.1.3 QIAprep® Spin Miniprep Kit

The QIAprep® Spin Miniprep Kit from Qiagen (Hilden, Germany) was used for the isolation of purified plasmid DNA as described in the manufacturer instruction.

3.2.2 Protocols (Standard molecular biological techniques)

3.2.2.1 Agarose Gel Electrophoresis

For the preparation of 1% agarose gels, 1 g agarose was added to 100 ml 1 x TAE buffer. The agarose gel was heated for 2minutes in the microwave until the agarose was dissolved. At last 1µl of SYBR® safe DNA Gel stain was added and the gel was framed for 30 minutes.
The samples were mixed with 5 x Loading Dye before they were pipetted into the slots of the gel. For the estimation and confirmation of the size of the DNA samples 7µl of DNA ladder Hyperladder-I was used. The electrophoresis was a run for ~30 minutes at 110 V voltage.

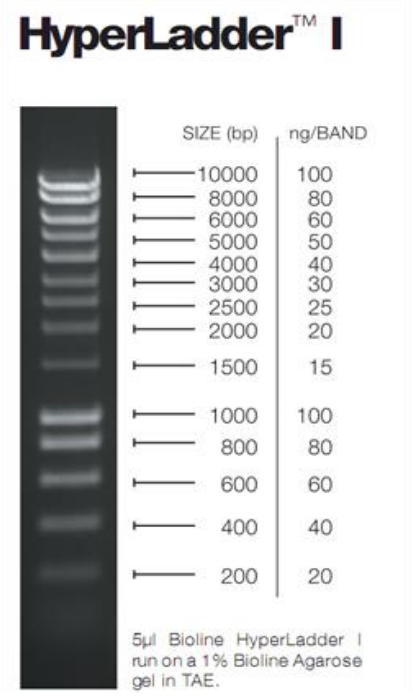

Figure 12 : Bands of the Hyperladder™I DNA ladder with corresponding sizes in base pairs.

3.2.2.2 PCR (Polymerase chain reaction)

PCR procedures were performed using Q5® Hot start DNA polymerase and Q5® DNA polymerase to amplify the gene of interest for further plasmid cloning. Components of the PCR reaction mixture are listed in Table 13. Table 14 shows the temperature program for the thermal cycler.

3.2.2.3 Adeno-associated virus Titration using qPCR

To quantify the virus concentration, Quantitative Polymerase Chain Reaction (qPCR) was performed. The reaction was set-up using TaqMan™ Fast virus 1-Step Master Mix (Applied Biosystems, Foster City, United States). To expose the virus genetic material for virus titration, proteinase K treatment was done in order to remove those proteins protecting the virus genetic material (DNA or RNA). 3µl viral sample, 6µl 5X Q5® reaction buffer, 6µl proteinase K and 15µl H2O were mixed and incubated for an hour at 50℃. Then 20 minutes at 95℃ followed by cooling down on ice for five minutes. Afterwards 10 µl TaqMan 2x Mix, 1µl WPRE probe and 4µl H_2O and 5µl the obtained sample from the previous step were mixed and prepared with two replicates each. qPCR was performed at 95℃ for 10 minutes, 34X (95℃/15 s, 60℃/60 s), and the fluorescence was measured at 60℃.
The qPCR quantification was done using serial dilution of AAV_Syn1_CPTX_Ruby2_WPRE_SV40 as the standard curve to these respective overexpression viruses.

3.2.2.4 Restriction endonuclease reactions

Each unit of the restriction enzyme (see Table 9) cut 1µg of DNA. The digestion reaction were incubated for a minimum of 2 hours to overnight at 37°C.

3.2.2.5 Ligation

The ligation reaction was a mixture of 100 ng cut vector, DNA in a molar ratio of 1:5, 1µl of T4 ligase buffer, 1µl of T4 ligase and filled up with ddH2O to a total volume of 20µl. The ligation reaction was incubated for 3 hours at 23°C and overnight at 16°C.

3.2.2.6 Transformation of NEB® Stable Competent *E. coli*

Transformation was done using 200µl of competent cells. *E. coli* cells are able to incorporate foreign DNA once their cell walls are altered, such cells are called competenet cells. The competent cells slowly thawed on ice for 10 minutes, further the plasmid DNA or ligated product was properly and gently mixed. The mixture of competent cells and plasmids were kept on ice for 30 minutes, following 45 seconds of heat shock at 42°C and 2 minutes of cooling on ice. Afterwards 1 ml of LB medium was added to the mixture and let the cells regenerate for 1 hour at 37°C and 500 rpm in the Thermomixer.
The appropriate selective agar plates with antibiotics were chosen for plating the cells. After regeneration, the mixture was centrifuged down at 3500 rpm for 5 minutes and 100µl of the supernatant were kept to resuspend the pellet, the rest of supernatant was discarded. The plates were incubated overnight at 37°C.

3.7.2.7 Plasmid DNA isolation from NEB® Stable Competent *E. coli*

The starter culture was inoculated for the transformation to agar plates and incubated in a shaker at 37°C overnight. Then, plasmid DNA was isolated using quick start protocol of QIAprep® Spin Miniprep Kit.

3.2.2.8 Adeno-associated virus production with ongoing HEK-293T cells

On the first day, the ongoing passage of HEK cells was split to have two Petri dishes each with 6 million cells per virus preparation. On the second day, cells had a confluence of 75-82% of the total surface, which was enough for the transfection with the plasmids mixture (see Figure 15). For two Petri dishes, 3 ml of the solution A and solution B were mixed and incubated for 8-12 hours. 20 ml of pre-warm Isocov's medium with 4-10% FBS additive were used to replace the media on the third day. 9 ml of pre-warm PBS were added to harvest the cells on day four. The collected cells were harvested by centrifugation at 4°C and 1000 rpm for 10 minutes. Following 5 ml of buffer A addition, cells were freeze-thaw three times. For this purpose, 1µl of benzonase nuclease was added and the cells were incubated for an hour in a water bath at 37°C. Cells were spun down for 20 minutes at 4°C and 4000 rpm and the supernatant was purified using a 0.2 micron filter.
Further, the viral supernatant was passed through a pre-equilibrated heparin column and the column was loaded with 20 ml wash buffer plus 1,5 ml wash buffer 2 and 6 ml elution buffer. The eluate had its buffer exchanged with PBS. Using a concentrator, the eluate concentrated down to 250µl. 250µl of PBS were added to the eluate in order to end up with a final volume of 500µl of viruses. Finally, viruses were aliquoted to 10µl under a sterile bench.

3.2.3 In vitro cell culture

3.2.3.1 Plating of hippocampal primary neurons

Two technical assistants Katrin Böhm and Jenny Schneeberg prepared the cultures and hippocampal primary cells, respectively. Cultures were maintained in 12 well plates containing glass coverslips, which were coated with Polyethylenimine 0.1% (PEI). Coated plates were incubated in a CO_2 incubator for 90 minutes and underwent proper rinsing steps using autoclaved water. Glass coverslips were washed thoroughly four times to remove PEI. In the last washing step, the cells were additionally incubated for 30minutes.
To maintain the osmolarity for the further plating process, glass coverslips were washed off with DMEM. Each well should contain 150,000 cells, therefore the total number of cells required for 12 wells were calculated and mixed with pre-warm and pre-equilibrated DMEM+. After 3 hours of incubation, DMEM+ was discarded entirely. Wells were refilled with 1 ml of the mixed media (NB+ and conditional media).

3.2.3.2 Genotyping

Dr. Renato Frischknecht kindly provided the transgenic Thy1 EGFPxNeurotrypsin-deficient mouse line. Further, mice were crossbred with Thy1 EGF wild type mice at DZNE and the embryos were genotyped using Kapa Mouse Genotyping Hotstart kit (PEQLAB, Erlangen, Germany) with technical assistance of Katrin Böhm. Genotyping provided us with information that enables us to distinguish neurotrypsin-deficient mice (transgenic mice) from wild-type mice.

3.2.3.3 Maintaining the cell line

On day in vitro 7 (DIV7), cells were transfected with the viral vector. The amount of viruses to be transfected was calculated by its titer, 1µl AAV-Syn-Sec(CPTX)_Agrin22_Scarlet and 1.5µl AAV-Syn-Sec(CPTX)_Agrin15_Scarlet were added to the culture.
On DIV14,150-200 µl of fresh NB+ media were added to each well to prevent toxification.
The cultures were monitored between DIV15-21 and on DIV19 cultures were fixated.

3.2.3.4 Immunocytochemistry

For fixation, the cultures were exposed to PFA for 7 minutes. The coverslips were washed three times of with cold PBS, 5 minutes each, followed by 10 minutes of permeabilization. Cover slips were washed with permeabilization buffer (Table 7) three times after 5 minutes incubation. Prior to antibody application, coverslips were incubated 1 hour in a blocking buffer (Table 7). Immunostaining was done incubating coverslips overnight at 4℃ after the primary antibodies were added with an adequate dilution factor (Table 11).
On the next day, primary antibodies were removed from coverslips by means of three PBS washes each lasting 5minutes. Then cover slips were incubated with the secondary antibody (Table 12) dilution for one hour at room temperature.
Finally, coverslips were directly taken and turned over and put onto glass slips with a drop of mounting media. During all steps of immunocytochemistry coverslips were protected from light exposure to prevent bleaching of the dye.

3.3 Confocal laser scan microscopy

All images were acquired using a Carl Zeiss Laser Scanning Microscope 700 (Carl Zeiss AG, Jena, Germany) whereby customized acquisition settings were used in the ZEN (Carl Zeiss AG, Jena, Germany). Pictures were taken using a 63x oil immersion objective. ’Frame’ size was 512x512 pixels and grey values had 8-bit resolution. Optical sections were obtained along the z-axis where the number of the slices varied between 8-10, which corresponds to 0.50µm Z resolution and at a zoom of 1.
The confocal microscopy was done in three different regions of each coverslip. Since neurons tend to be more aggregated in the central region and neurons at the margin are more scattered, three measuring spots were chosen near the border of the coverslip. The border of coverslips was chosen because of the lower abundance of the neuronal population as well as synaptic density which it eased the synaptic density quantification.

3.4 Image processing and quantification

Image analysis was done using ZEN (Carl Zeiss AG, Jena, Germany) and ImageJ (National Institute of Health, Maryland, United States). A specific plug-in of ImageJ, SynPuCo/Synapse counter (Egor Dzyubenko and Andrey Rozenberg) was used to quantify synaptic puncta. The maximal intensity projection of images underwent image processing. The default parameters of this plug-in were used with RenylEntropy as the appropriate method for thresholding. The total area occupied by dendrites in an image, the mean and maximal intensity of the whole image were measured to estimate the density of the dendritic area (DA).
The dendritic area was calculated using the below formula:

DA= Mean Intensity / Thy1-eGFP area or total area * Max intensity

For all the images the measured total area occupied by dendrites and its maximal intensity were 10325.5µm^2 and 255, respectively. The results correspond to counts of the presynaptic, postsynaptic and co-localized puncta. Finally, the synaptic density was estimated by normalizing the number of presynaptic, postsynaptic and co-localized puncta relative to the density of dendritic area.

3.5 Statistics

Statistical analysis was performed using GraphPad Prism software. Data were tested for a significant difference by executing t-tests – unpaired and nonparametric analyses. The differences between groups were regarded as significantly different for p values smaller than 0.05.

4. RESULTS

4.1 Characterization of COOH-terminal domain of Agrin

Previous studies demonstrated the prominent role of C-Ag22kDa fragment in spinogenesis and synaptogenesis (Koulen, Honig, Fletcher, & Kröger, 1999; Ksiazek et al., 2007). The C-Ag22kDa has been shown to be sufficient fragment for normal neuronal activity (Hoover et al., 2003).

In my thesis, I studied the function of Agrin C-Ag22kDa and C-Ag15kDa (control) fragments by means of overexpression adeno-associated viruses. The expression was examined in wild-type and neurotrypsin-knock out neuronal cultures from the mouse hippocampus.

4.2 Quantification of overexpression adeno-associated virus

To quantify the concentration of produced viruses (3.1.2), qPCR was performed (3.7.2.3) and the result is shown in Table 4 and Figure 13. For this purpose, the serial dilution of AAV_Syn1_CPTX_Ruby2_WPRE_SV40 served as a standard curve to compare with prepared overexpression viruses, whereby each dilution was prepared two times.

Table 4: Titration values measured by qPCR.

The standard curve plotted according to the values of the following table:

Sample	ΔCt	2^-CT	Plasmid copies	Plasmid MW*	Weight (ng)*
0,0001	25,365	2,31328E-08	1,47E+04	6,80E-18	1,00E-13
0,001	23,731	7,18256E-08	1,47E+05	6,80E-18	1,00E-12
0,01	18,002	3,81022E-06	1,47E+06	6,80E-18	1,00E-11

0,1	15,832	1,71452E-05	1,47E+07	6,80E-18	1,00E-12
1	14,782	3,54948E-05	1,47E+08	6,80E-18	1,00E-13

*Plasmid weight in nanogram and molecular weight used to calculate the plasmid dilution.

The Ct (Cycle Threshold) value is defined as number of the cycles required for the fluorescence signals to cross the threshold. For the technical replicates, the Ct values were averaged.

The table below lists the quantified virus after the lysate filtration (Filtered), purification (Purified) and elution (Eluted) step of virus preparation.

Sample	ΔCt	2^-CT	Plasmid copies	Dilution 1/10 (Particles/ µl)	Titer (Particles/ml)
Agrin22 Filtered	16.184	0.0000134285	1.34E+0	1.34E+08	1.34E+11
Agrin22 Purified	22.884	0.0000001291	1.29E+05	1.29E+06	1.29E+09
Agrin22 Eluted	16.768	0.0000089552	8.96E+06	8.96E+07	8.96E+10
Agrin22	15.117	0.0000281249	2.81E+07	2.81E+08	2.81E+11
Agrin15 Filtered	14.562	0.0000413268	4.13E+07	4.13E+08	4.13E+11
Agrin15 Purified	20.990	0.0000004799	4.80E+05	4.80E+06	4.80E+09
Agrin15 Eluted	15.363	0.0000004799	2.37E+07	2.37E+08	2.37E+11
Agrin15	15.729	0.0000184063	1.84E+07	1.84E+08	1.84E+11

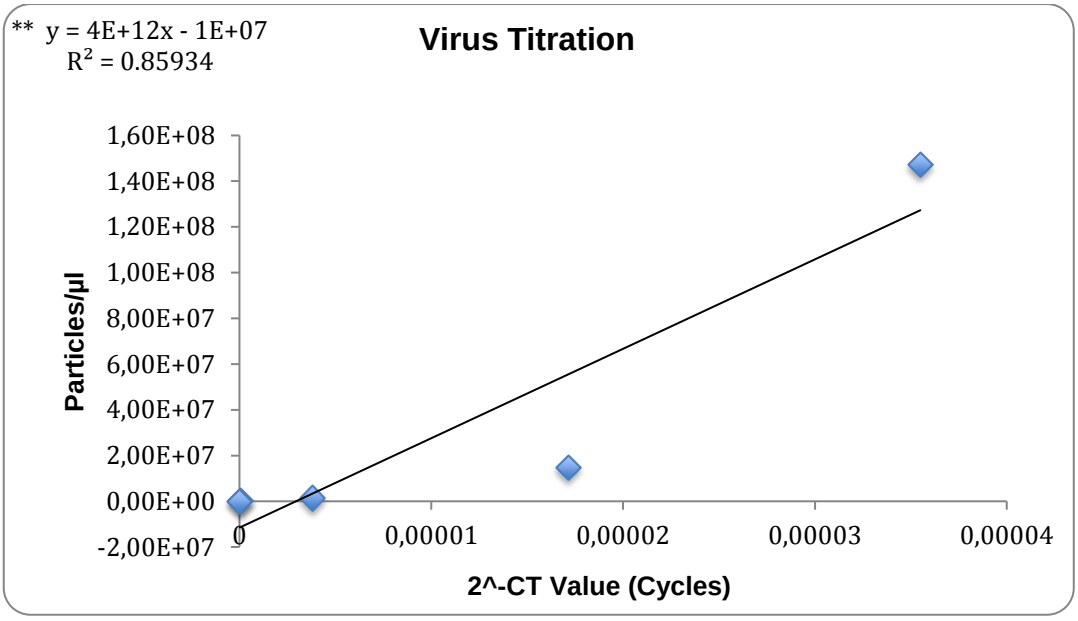

Figure 13: Power quantification result of AAV_Synapsin_SecretionSequence(CPTX)_Agrin22_Scarlet And AAV_Synapsin_SecretionSequence(CPTX)_Agrin15_Scarlet. This figure illustrates the regression line derived from plasmid dilution (genomes /µl). The blue points represents the calibrator/standard values.

According to the titration result AAV_Synapsin_SecretionSequence(CPTX)_ Agrin22_Scarlet had a higher titer than the AAV_Synapsin_ SecretionSequence(CPTX)_Agrin15_Scarlet. Hence, Agrin15 power had to be equalized to Agrin22 power in order to guarantee a similar infection effect in both groups. Therefore, 1µl of Agrin22 and 1.5 µl of Agrin15 viruses were used for *in vitro* infection.

4.3 Immunostaining of Agrin-22/15-infected culture and the ‘ Crosstalk ‘ phenomenon

The Glutamergic neuron marker VGlut1 was used as presynaptic marker and Homer as postsynaptic marker, which their secondary antibodies detect them. Immunostaining faced a ‘ crosstalk ‘ phenomenon between emitted signals from Alexa Flour 594 (Agrin-22/15-scarlet tagged) and Alexa Flour 633 (the presynaptic marker). As Alexa flour 594 spectra partially overlaps with Alexa flour 633, the mScarlet/Alexa flour 594-emission signal transmitted on this channel was cross-talked with the signal emitted from Alexa flour 633 (see Figure 14).

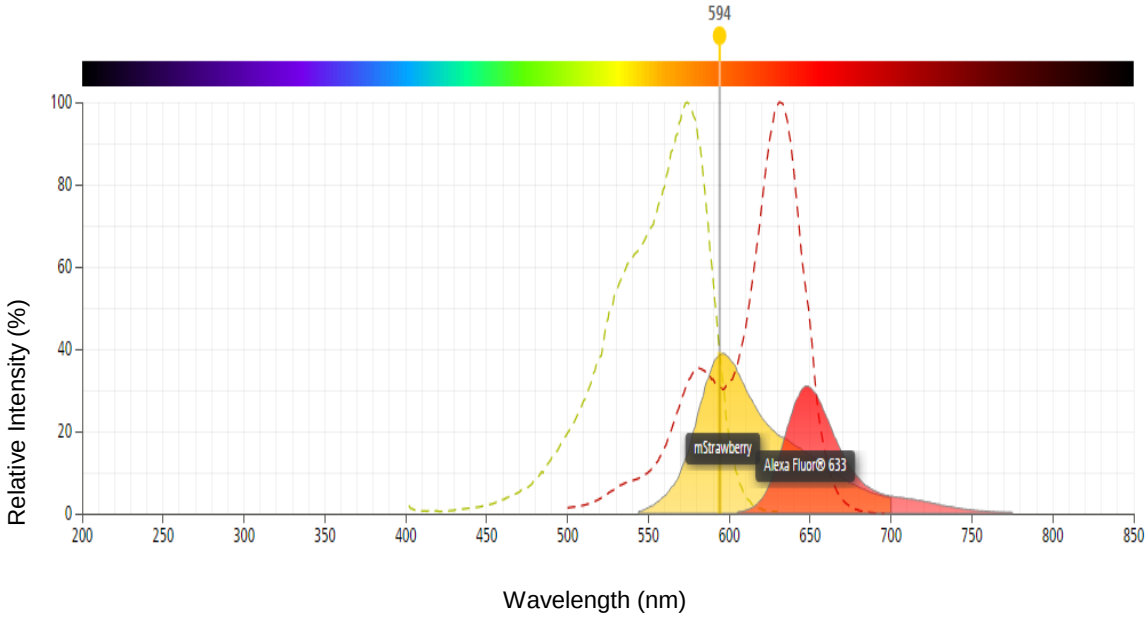

Figure 14: Spectral properties of fluorescence dyes. **Absorbance spectra of Alexa flour 594 and 633 (dotted lines)**. mStrawberry/Alexa flour 594 and Alexa flour 633 fluorescence emission is shown in yellow and red colors, respectively. The cross-talk effect occurred in the range between 600nm and 700nm arising from the spectral overlap between Alexa flour 594 and 633.

The pictures shown in figure 15 resulted from the additional control staining, to distinguish between both spectra of mStrawberry/Alexa flour 594 and Alexa flour 633. The control detected the precise signal from the Agrin22/15 channel in the absence of the VGlut1 marker (Figure 15).
The negative control of the staining revealed the true emission caused by the VGlut1 marker in uninfected coverslips, this confirmed that the marker is functional and that there is no false signal stemming from the Agrin channel.

A

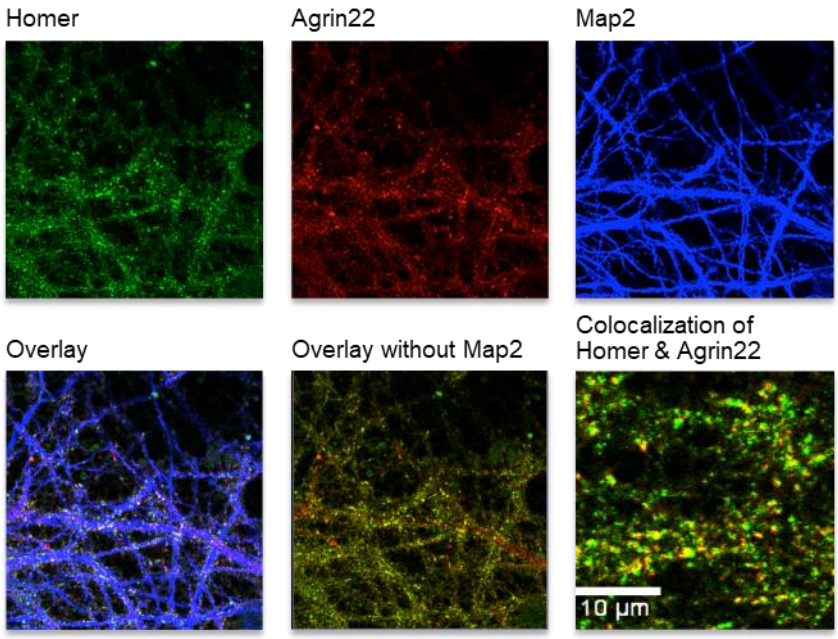

B

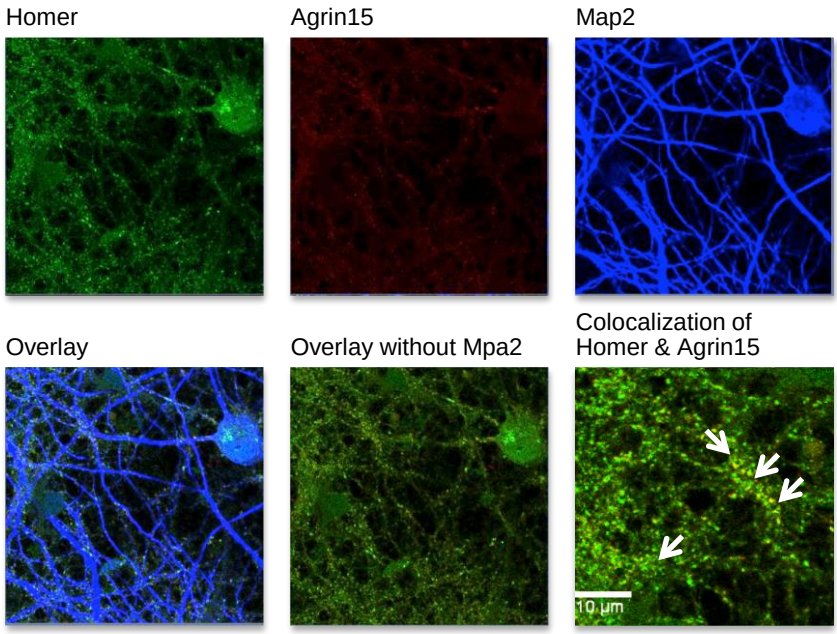

Figure 15: Agrin22 and Agrin15 expression in the absence of VGlutI (Presynaptic marker). The MAP2 (Microtubule Associated Protein2) antibody is used to track down the neuron shape/structure. (A) Shows the expression of Agrin22 in the absence of the VGlutI marker. (B) Shows the expression of Agrin15 in the absence of the VGlutI marker. Absence of VGlutI marker and the presence of its secondary antibody (Alexa flour 633) in this control staining, displayed the exact signal from Agrin expression. Arrows point out the overlapped puncta of postsynaptic marker (Homer) and Agrin22/15, which confirms the co-localization of Agrin at postsynaptic terminals.

4.4 Validation of Agrin-22 and Agrin-15 in wild-type cultures

To characterize the respective viruses in the wild-type culture, 3 replicates of wild-type cultures were infected. Microscopic inspection of the wild-type culture showed healthy conditions and an appropriate expression of the virus.
A quantitative evaluation of how AAV-Ag22 and -Ag15 expressions modified the synaptic density is still lacking. This paucity was due to the rather small number of immunostained coverslips. The figure 16 and 17 show the characterization of Agrin22-infected and Agrin15-infected, respectively and also the co-localisation of the presynaptic marker (VGlutI) and postsynaptic marker (Homer).

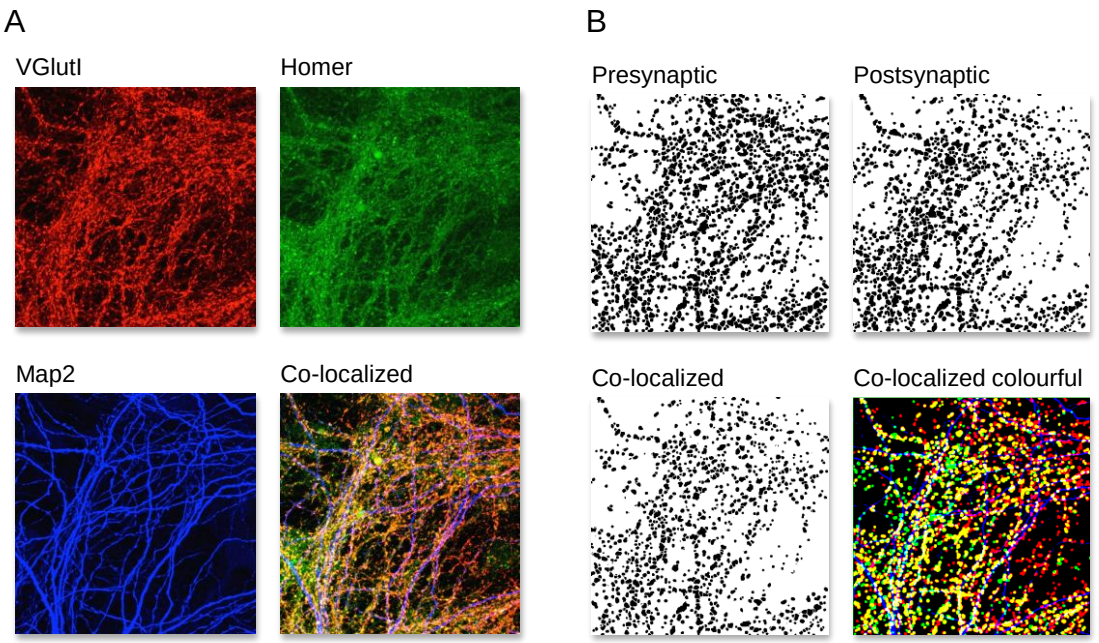

Figure 16: Agrin22-infected neurons from the wild-type culture. Co-localized image of VGultI and Homer spots synapses. (A) Confocal Images of Agrin22-transfected neurons. (B) The output images after processing A with the synapse counter plug-in reveals the density of synapses.

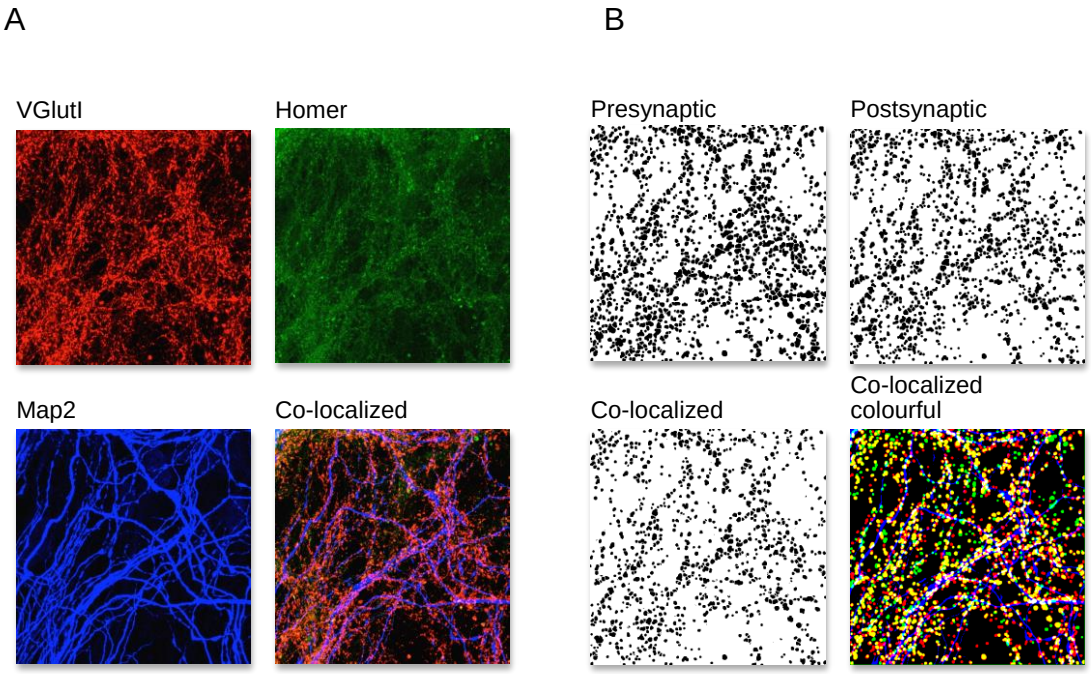

Figure 17: Agrin15-infected neurons from the wild-type culture. (A) Confocal Images of Agrin15-transfected neurons. (B) The output images after processing A with synapse counter plug-in.

The quantitative result of synaptic density was obtained by counting the presynaptic, postsynaptic and co-localized puncta per dendritic area. Due to a rather low sample size of N=9, the qualitative analysis of synaptic density failed to show a significant difference between the wild-type cultures infected with Agrin22 or Agrin15 viruses ($p > 0.05$, unpaired T-test). Figure 18 shows the average synaptic density of both groups.

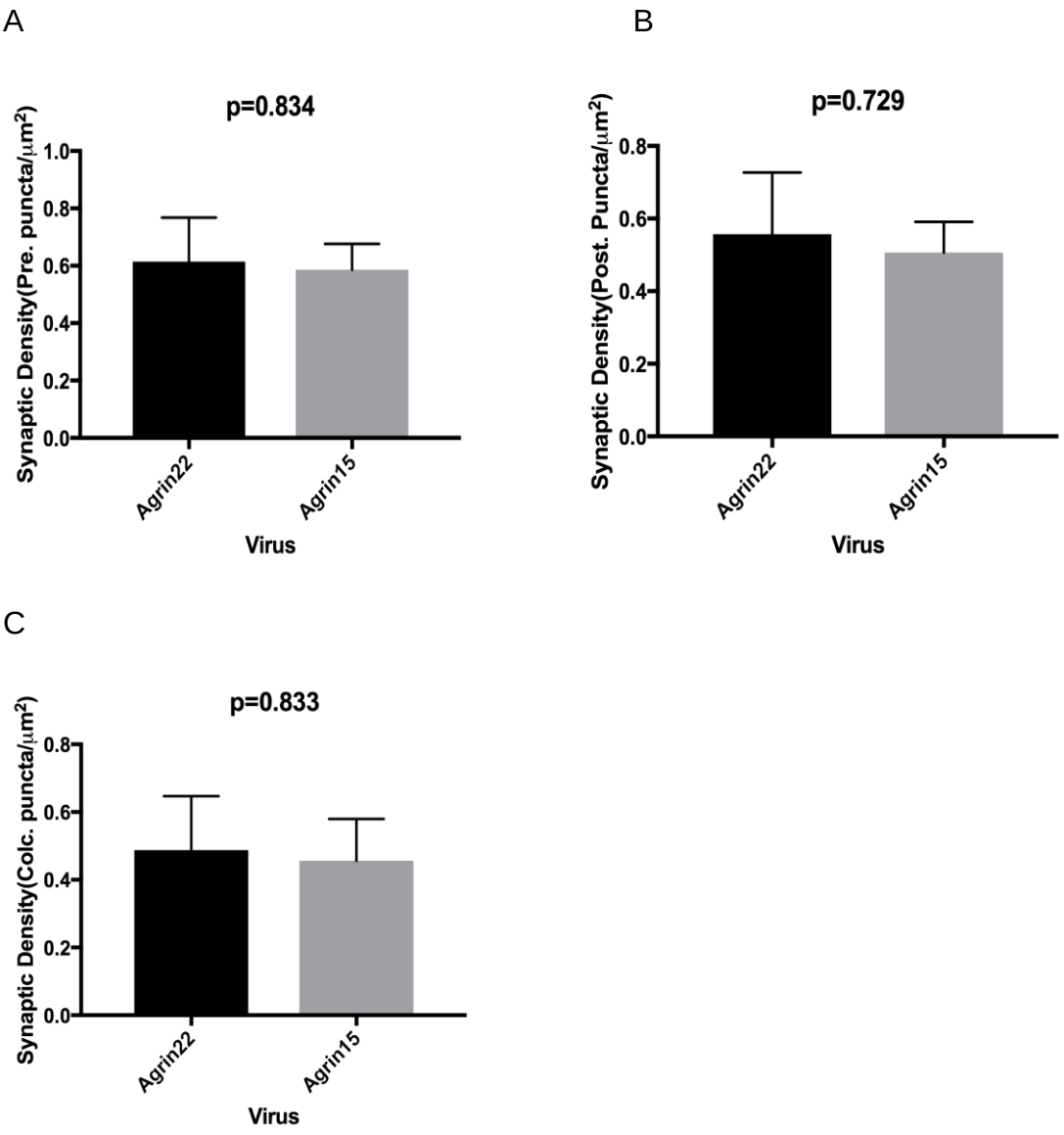

Figure 18: Average synaptic density per dendritic area A) Counts of presynaptic puncta per dendritic area (B) Counts of postsynaptic puncta per dendritic area, (C) Counts of co-localized puncta per dendritic area. The statistical analysis from Agrin22 and Agrin15-infected neurotrypsin-deficient cultures showed no significant difference between both groups. The synaptic density measurement was tested for a significant difference between groups using unpaired T-test.

4.5 Validation of Agrin-22 and Agrin-15 in the neurotrypsin-deficient culture

Unfortunately, two rounds of neurotrypsin-knock out cultures had to be withdrawn due to unhealthy cultures. However, data from section 4.4 previously validated that infection with the respective viruses in the wild-type culture was successful. The quantification of immunostaining was possible in the third replicate of Agrin22- and Agrin-15-infected cultures. The neurotrypsin-knockout neuron cultures were prepared from the hippocampus of Thy1-eGFP mice, whereby the excitatory neurons were tagged with eGFP. In order to spot the location of synapse upon the excitatory dendrites, VGlutI and Homer were used as presynaptic and postsynaptic marker, respectively. Figure 19 and 20 shows the staining of Agrin22-infected and Agrin15-neurons from neurotrypsin-knockout culture, respectively. Figures display the density of presynaptic (VGlutI), postsynaptic (Homer) and co-localisation of both vesicles.

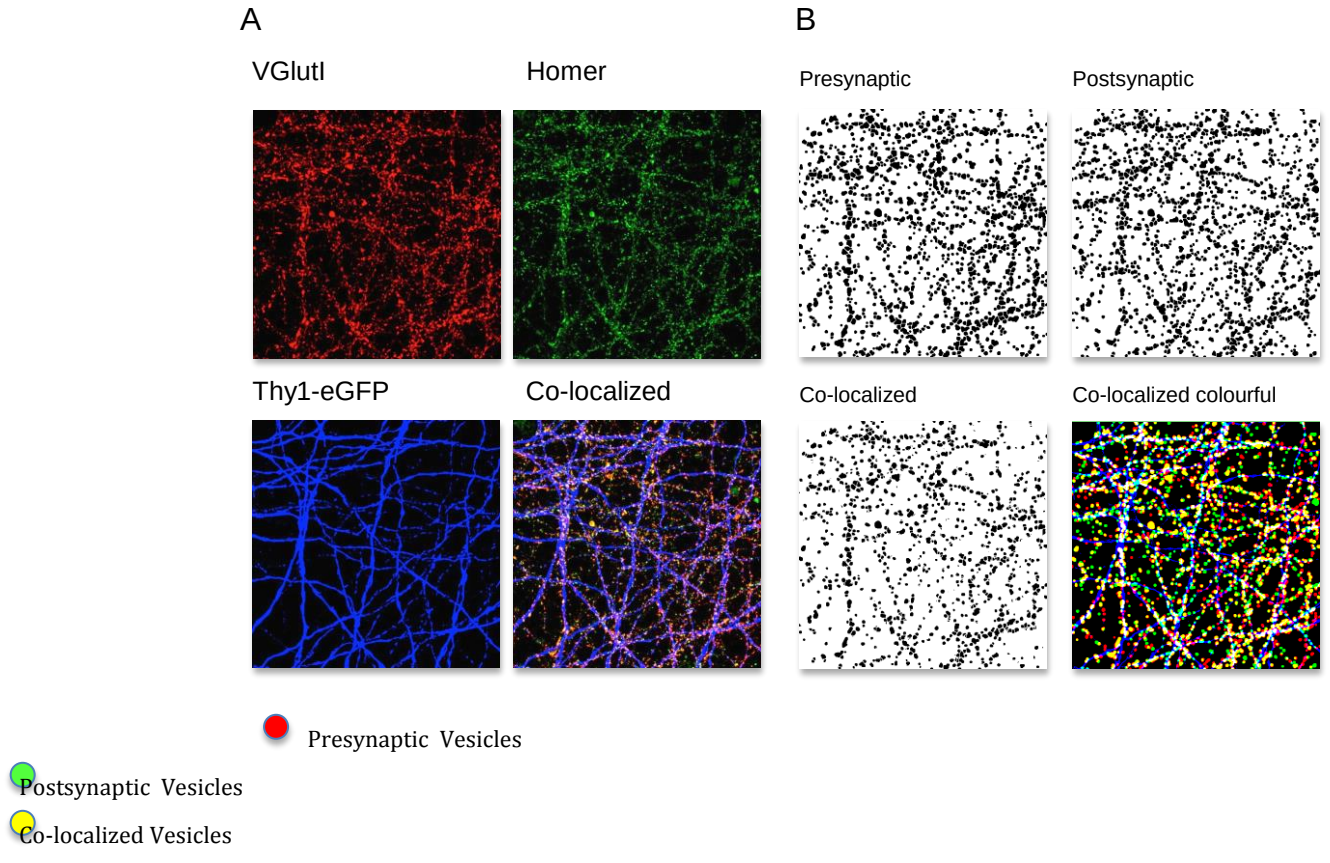

Figure 19: Agrin-22-infected neurons from neurotrypsin-knockout culture. (A) Confocal images of Agrin22-transfected neurons. (B) The output images after processing A with the synapse counter plug-in.

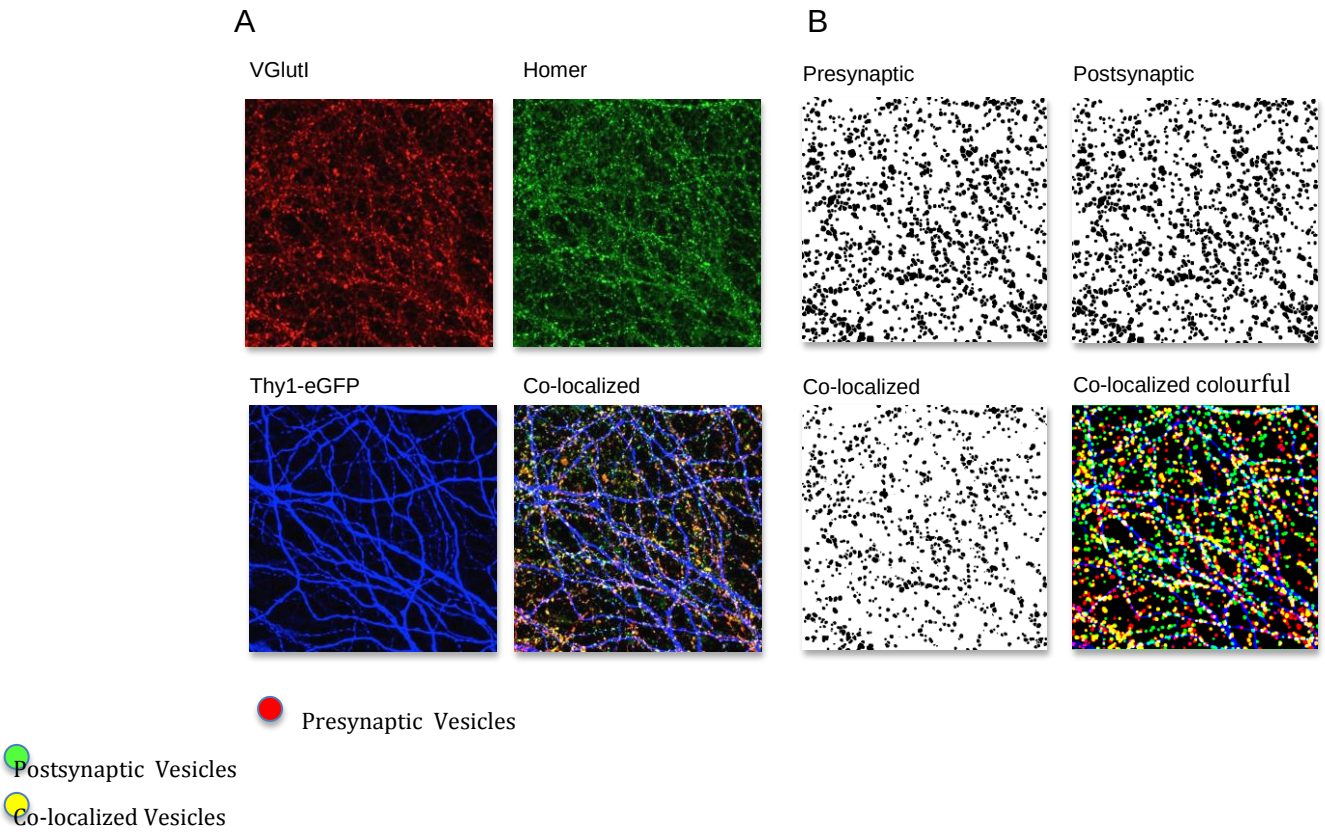

Figure 20: Agrin-15-infected neurons from neurotrypsin-knockout culture. (A) Confocal Images of Agrin15-transfected neurons. (B) The output images after processing A with synapse counter plug-in.

Due to the low sample size of N=9, the qualitative measurements failed to show a significant difference between Agrin22-infected and Agrin15-infected neurotrypsin-knockout neuron cultures. Figure 21 shows the average synaptic density of both groups.

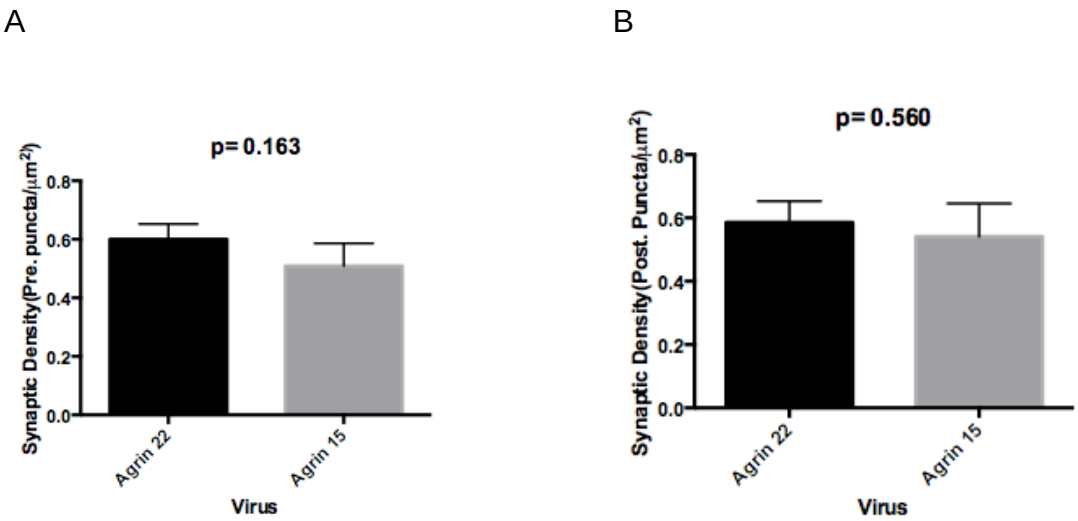

C

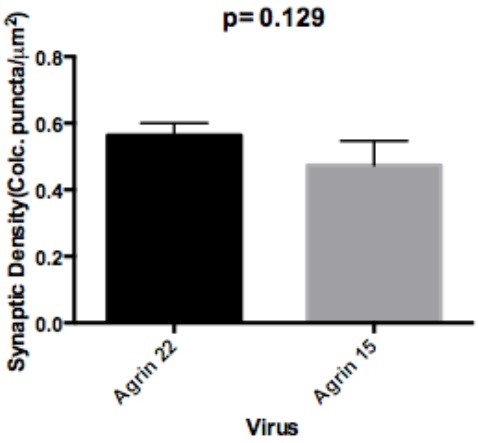

Figure 21: Comparison of the synaptic density between Agrin22- and Agrin15-infected neurotrypsin-knockout cultures. (A) Count of presynaptic puncta per dendritic area, (B) Count of postsynaptic puncta per dendritic area, (C) Count of co-localized puncta per dendritic area.

In summary, the results of this study demonstrate a difference between the expression rate of AAV-Ag22 and -Ag15 in neuronal cultures. Surprisingly, the expression of AAV-Ag22 was higher than AAV-Ag15, despite the fact that AAV-Ag22 and -Ag15 was added in cultures at the same amount. However, my thesis failed to demonstrate the effect of C-Agrin22kDa and its competitive antagonist (C-Agrin15kDa) via AAV expression.

5. DISCUSSION

Characterization of the COOH-terminal domain of Agrin

The neurotrypsin-dependent cleavage of Agrin has been tested by administration of 110kDa, 90kDa and 22kDa fragments of Agrin in neurotrypsin-deficient mice. Agrin-110 showed an insignificant and weak rescue and Agrin-90 was unable to rescue the filopodial response and synapse formation. Interestingly, Agrin22 administration mediates a significant effect on filopodial response (Matsumoto-Miyai et al., 2009). Several studies demonstrated the prominent role of the C-Ag22kDa fragment in the CNS (Koulen et al., 1999; Ksiazek et al., 2007) and it has been shown to be sufficient for normal neuronal activity (Hoover et al., 2003).

The C-Ag22kDa serves as a potential mediator in LTP-associated synapse development

It is commonly accepted that dendritic filopodia serve as precursors for spinogenesis, which is the precursor of activity-dependent synaptogenesis (Zito, Knott, Shepherd, Shenolikar, & Svoboda, 2004). Previous research revealed a crucial role of neurotrypsin-dependent cleavage of Agrin at synapses, with major implications for dendritic filopodia development (Matsumoto-Miyai et al., 2009). Moreover, Hilgenberg et al. has previously shown that Agrin-signaling enhances those neuronal responses that release neurotransmitters at excitatory synapses (Hilgenberg, Ho, Lee, O'Dowd, & Smith, 2002). In addition, the Agrin loss selectively influences excitatory but not inhibitory synapses (Ksiazek et al., 2007). This distrupts LTP and thereby alters important cognitive tasks, majorly memory formation and learning (Lynch, 2004; Okano, Hirano, & Balaban, 2000). This is the first study that generates further insight into the characterization of C-Ag22kDa via AAV expression. I was able to express both fragments in neuro-trypsin deficient hippocampal neurons and record its effect on synapse formation. Future *in vivo* and behavioral studies using this AAV technology in neurotrypsin-deficient mice will reveal data that allows gaining insights into the functional role of the Ag22kDa fragment of agrin.

Is the C-Ag15kDa fragment a competitive inhibitor of C-Ag22kDa?

Data from several studies showed the administration ofC-Ag15kDa blocks the binding of C-Ag22kDa with little effect on the Na^+ level of resting neurons but it disrupted the normal enhancement caused by C-Ag22kDa (Hilgenberg et al., n.d.). Consistent with the previous observation of Hilgenberg et al., C-Ag15kDa was found to be effective at inhibiting the depolarization triggered by the C-Ag22kDa via a small hyperpolarization. In light of these results, C-Ag15kDa served as the antagonist of C-Ag22kDa, and control fragment for this study.

In my thesis, I cloned the C-Ag22kDa and C-Ag15kDa (control) fragments into overexpression AAV-based vectors, and further used the respective vectors to produce AAVs. Afterwards, I performed the *in vitro* validation of the prepared AAVs in the wild type and neurotrypsin-knock out neuronal cultures from the

mouse hippocampus. Finally, I was able to study the function of C-Ag22kDa and its prospective antagonist C-Ag15kDa by examining the expression of the AAVs in either of the cultures (wild-type and neurotrypsin-knock out). However, the available neuron cultures were limited and the results are not significant due to a low sample size. In the future, sets of optimizations have to be implemented and change the presented outcome. The main reason for unhealthy neurotrypsin-deficient cultures remained unclear. The most probable reason for cell death could be inappropriate coating and cunctation of plating while waiting for the genotyping result, which was necessary to have an understanding of the type of the mice. In addition, the results shown in Figure 21 were obtained from suboptimal cultures (neurotrypsin-deficient culture), which were obvious, by the disappearance of already established communications among surviving cells. Therefore, it seems that this culture is not a valid model for testing the effect of Agrin fragments on synapse formation.

Finally, I was able to study the function of C-Ag22kDa and its antagonist (C-Ag15kDa) on synapse formation by examining the expression of the AAVs in either of the cultures (wild-type and neurotrypsin-knock out). The result from this experiment demonstrates that C-Ag22kDa and C-Ag15kDa AAVs were extensively expressed in both neuron cultures. However, C-Ag15kDa AAV expression was found to infect the neuronal culture less than C-Ag22kDa AAV. One reason could be that AAV-Ag15 expression is less stable. Another possibility is that administration of C-Ag15kDa peptide is less stable in the culture than the C-Ag22kDa fragment. The structural study of C-Ag22kDa showed that this might happen since the C-Ag22kDa fragment is degraded through a normal physiological mechanism (neurotrypsin-dependent cleavage) in the CNS, whereas C-Ag15kDa was only applied exogenously.

Is $\alpha 3$NKA a neuronal receptor for Agrin?

Hilgenberg and co-workers have already speculated that C-Ag22kDa binds to the $\alpha 3$ subunit of the sodium-potassium ATPase (NKA) in neurons of the CNS proposing it as the neuronal receptor for Agrin (Hilgenberg et al., 2006). However, the precise location remains to be identified. Future *in vivo* studies are necessary to investigate the exact location of the dendritic receptor mediating the filopodia–inducing function of C-Ag22kDa. Therefore, the additional optimization can be done to enhance the binding rate of C-Ag22kDa to its receptor. Therapeutically, this knowledge offers a potential treatment of patients suffering from a deficit in memory and learning, such as Amnesia.

6. REFERENCES

Ben Achour, S., & Pascual, O. (2010). Glia: The many ways to modulate

synaptic plasticity. *Neurochemistry International*, *57*(4), 440–445. https://doi.org/10.1016/j.neuint.2010.02.013
Blundon, J. A., & Zakharenko, S. S. (2008). Dissecting the Components of Long-Term Potentiation. *The Neuroscientist*, *14*(6), 598–608. https://doi.org/10.1177/1073858408320643
Bonneh-Barkay, D., & Wiley, C. A. (2009). Brain extracellular matrix in neurodegeneration. *Brain Pathology (Zurich, Switzerland)*, *19*(4), 573–85. https://doi.org/10.1111/j.1750-3639.2008.00195.x
Bose, C. M., Qiu, D., Bergamaschi, A., Gravante, B., Bossi, M., Villa, A., … Ruegg, M. A. (2000). Agrin controls synaptic differentiation in hippocampal neurons. *The Journal of Neuroscience : The Official Journal of the Society for Neuroscience*, *20*(24), 9086–95. https://doi.org/10.1523/jneurosci.1609-07.2007
Carey, D. J. (1997). Syndecans : multifunctional cell-surface co-receptors. *Biochem. J*, *327*, 1–16. Retrieved from https://www.ncbi.nlm.nih.gov/pmc/articles/PMC1218755/pdf/9355727.pdf
Cherubini, E., & Miles, R. (2015). The CA3 region of the hippocampus: how is it? What is it for? How does it do it? *Frontiers in Cellular Neuroscience*, *9*, 19. https://doi.org/10.3389/fncel.2015.00019
Clegg, D. O., Wingerd, K. L., Hikita, S. T., & Tolhurst, E. C. (2003). Integrins in the development, function and dysfunction of the nervous system. *Frontiers in Bioscience : A Journal and Virtual Library*, *8*, d723-50. Retrieved from http://www.ncbi.nlm.nih.gov/pubmed/12700040
Cleva, R. M., Gass, J. T., Widholm, J. J., & Olive, M. F. (2010). Glutamatergic targets for enhancing extinction learning in drug addiction. *Current Neuropharmacology*, *8*(4), 394–408. https://doi.org/10.2174/157015910793358169
Daniels, M. P. (2012). The role of agrin in synaptic development, plasticity and signaling in the central nervous system. *Neurochemistry International*, *61*(6), 848–53. https://doi.org/10.1016/j.neuint.2012.02.028
Dityatev, A., & Schachner, M. (2003). Extracellular matrix molecules and synaptic plasticity. *Nature Reviews Neuroscience*, *4*(6), 456–468. https://doi.org/10.1038/nrn1115
Dityatev, A., Schachner, M., & Sonderegger, P. (2010). The dual role of the extracellular matrix in synaptic plasticity and homeostasis. *Nature Reviews Neuroscience*, *11*(11), 735–746. https://doi.org/10.1038/nrn2898
Dityatev, A., Wehrle-Haller, B., & Pitkänen, A. (n.d.). *Brain extracellular matrix in health and disease*. Retrieved from https://books.google.de/books?id=SMoSBAAAQBAJ&pg=PA112&lpg=PA112&dq=Agrin+extracellular+matrix+brain&source=bl&ots=tg6I-KFeX7&sig=ucKz4-vnZ5IuyCqLr4Agho4iLh4&hl=en&sa=X&ved=0ahUKEwjCn8_n7rnXAhXRDOwKHfR9BpoQ6AEITjAJ#v=onepage&q=Agrin extracellular matrix brain&f=false
Eichenbaum, H., & Cohen, N. J. (2001). (2001). From conditioning to conscious recollection: Memory systems of the brain. *Oxford Psychology Series*, *no.35*. Retrieved from http://psycnet.apa.org/record/2001-06744-000
Ethell, I. M., & Yamaguchi, Y. (1999). Cell surface heparan sulfate proteoglycan syndecan-2 induces the maturation of dendritic spines in rat

hippocampal neurons. *The Journal of Cell Biology*, *144*(3), 575–86. Retrieved from http://www.ncbi.nlm.nih.gov/pubmed/9971750
Eysenck, M. W. (2012). *Fundamentals of cognition*. Psychology Press.
Florian, C., & Roullet, P. (2004). Hippocampal CA3-region is crucial for acquisition and memory consolidation in Morris water maze task in mice. *Behavioural Brain Research*, *154*(2), 365–374. https://doi.org/10.1016/j.bbr.2004.03.003
Foerde, K., & Poldrack, R. A. (2009). Procedural learning in humans. In L. R. Squire (Ed.), The new encyclopedia of neuroscience, Vol. 7 (pp. 1083-1091). Oxford, UK: Academic Press. - Google Search. (n.d.). Retrieved December 2, 2017, from https://www.google.de/search?source=hp&ei=KQQjWq36NIzWwAKRqqqoBw&q=Foerde%2C+K.%2C+%26+Poldrack%2C+R.+A.+%282009%29.+Procedural+learning+in+humans.+In+L.+R.+Squire+%28Ed.%29%2C+The+new+encyclopedia+of+neuroscience%2C+Vol.+7+%28pp.+1083-1091%29.+Oxford%2C+
Frischknecht, R., Fejtova, A., Viesti, M., Stephan, A., & Sonderegger, P. (2008). Activity-induced synaptic capture and exocytosis of the neuronal serine protease neurotrypsin. *The Journal of Neuroscience : The Official Journal of the Society for Neuroscience*, *28*(7), 1568–79. https://doi.org/10.1523/JNEUROSCI.3398-07.2008
Garcia-Osta, A., Tsokas, P., Pollonini, G., Landau, E. M., Blitzer, R., & Alberini, C. M. (2006). MuSK Expressed in the Brain Mediates Cholinergic Responses, Synaptic Plasticity, and Memory Formation. *Journal of Neuroscience*, *26*(30), 7919–7932. https://doi.org/10.1523/JNEUROSCI.1674-06.2006
Goda, Y., & Stevens, C. F. (1996). Synaptic plasticity: the basis of particular types of learning. *Current Biology : CB*, *6*(4), 375–8. https://doi.org/10.1016/S0960-9822(02)00499-2
Harburger, D. S., & Calderwood, D. A. (2009). Integrin signalling at a glance. *Journal of Cell Science*, *122*(Pt 2), 159–63. https://doi.org/10.1242/jcs.018093
Hilgenberg, L. G. W., Ho, K. D., Lee, D., O'Dowd, D. K., & Smith, M. A. (2002). Agrin Regulates Neuronal Responses to Excitatory Neurotransmitters in Vitro and in Vivo. *Molecular and Cellular Neuroscience*, *19*(1), 97–110. https://doi.org/10.1006/mcne.2001.1056
Hilgenberg, L. G. W., Su, H., Gu, H., O'Dowd, D. K., & Smith, M. A. (2006). Alpha3Na+/K+-ATPase is a neuronal receptor for agrin. *Cell*, *125*(2), 359–69. https://doi.org/10.1016/j.cell.2006.01.052
Hilgenberg, L. G. W., Su, H., Gu, H., O 'dowd, D. K., & Smith, M. A. (n.d.). a3Na + /K + -ATPase Is a Neuronal Receptor for Agrin. https://doi.org/10.1016/j.cell.2006.01.052
Hoover, C. L., Hilgenberg, L. G. W., & Smith, M. A. (2003). The COOH-terminal domain of agrin signals via a synaptic receptor in central nervous system neurons. *The Journal of Cell Biology*, *161*(5), 923–32. https://doi.org/10.1083/jcb.200301013
Izumi, Y., & Zorumski, C. F. (2008). Direct cortical inputs erase long-term potentiation at Schaffer collateral synapses. *The Journal of Neuroscience : The Official Journal of the Society for Neuroscience*, *28*(38), 9557–63. https://doi.org/10.1523/JNEUROSCI.3346-08.2008

Kandel, E. R. (2001). The molecular biology of memory storage: A dialogue between gene and synapses. *Science*, *294*(5544), 1030–1038. https://doi.org/10.1126/science.1067020

Kauer, J. A., & Malenka, R. C. (2007). Synaptic plasticity and addiction. *Nature Reviews Neuroscience*, *8*(11), 844–858. https://doi.org/10.1038/nrn2234

Kayser, M. S., Nolt, M. J., & Dalva, M. B. (2008). EphB receptors couple dendritic filopodia motility to synapse formation. *Neuron*, *59*(1), 56–69. https://doi.org/10.1016/j.neuron.2008.05.007

Khan, Z. U., Muly, E. C., & Alkon, D. L. (n.d.). *Molecular basis of memory. Volume one hundred and twenty-two, Progress in molecular biology and translational science*. Retrieved from https://books.google.de/books?id=g4gpAgAAQBAJ&pg=PA1&lpg=PA1&dq=Molecular+Basis+of+Memory+Zafar+U.+Khan*†,+...+E.+Chris+Muly§¶%7C%7C,+in+Progress+in+Molecular+Biology+and+Translational+Science,+2014&source=bl&ots=4_0_Sc7agM&sig=NDj7yA-AVRZVLLceiSuKcHHYOQE&hl=en&sa=X&ved=0ahUKEwjMxubjprvXAhXQzKQKHRaiCdoQ6AEILzAC#v=onepage&q=Molecular Basis of Memory Zafar U. Khan*†%2C ... E. Chris Muly§¶%7C%7C%2C in Progress in Molecular Biology and Translational Science%2C 2014&f=false

Koudinov, a R., & Koudinova, N. V. (2001). Essential role for cholesterol in synaptic plasticity and neuronal degeneration. *The FASEB Journal : Official Publication of the Federation of American Societies for Experimental Biology*, *15*(10), 1858–1860. https://doi.org/10.1096/fj.00-0815fje

Koulen, P., Honig, L. S., Fletcher, E. L., & Kröger, S. (1999). Expression, distribution and ultrastructural localization of the synapse-organizing molecule agrin in the mature avian retina. *European Journal of Neuroscience*, *11*(12), 4188–4196. https://doi.org/10.1046/j.1460-9568.1999.00848.x

Ksiazek, I., Burkhardt, C., Lin, S., Seddik, R., Maj, M., Bezakova, G., … Ruegg, M. A. (2007). Synapse Loss in Cortex of Agrin-Deficient Mice after Genetic Rescue of Perinatal Death. *Journal of Neuroscience*, *27*(27), 7183–7195. https://doi.org/10.1523/JNEUROSCI.1609-07.2007

Lakhina, V., Arey, R. N., Kaletsky, R., Kauffman, A., Stein, G., Keyes, W., … Murphy, C. T. (2015). Genome-wide functional analysis of CREB/long-term memory-dependent transcription reveals distinct basal and memory gene expression programs. *Neuron*, *85*(2), 330–45. https://doi.org/10.1016/j.neuron.2014.12.029

Lau, L. W., Cua, R., Keough, M. B., Haylock-Jacobs, S., & Yong, V. W. (2013). Pathophysiology of the brain extracellular matrix: a new target for remyelination. *Nature Reviews Neuroscience*, *14*(10), 722–729. https://doi.org/10.1038/nrn3550

Li, J., Zelenin, S., Aperia, A., & Aizman, O. (2006). Low Doses of Ouabain Protect from Serum Deprivation-Triggered Apoptosis and Stimulate Kidney Cell Proliferation via Activation of NF- B. *Journal of the American Society of Nephrology*, *17*(7), 1848–1857. https://doi.org/10.1681/ASN.2005080894

Lin, J. B., Mast, N., Bederman, I. R., Li, Y., Brunengraber, H., Björkhem, I., &

Pikuleva, I. A. (2016). Cholesterol in mouse retina originates primarily from in situ de novo biosynthesis. *Journal of Lipid Research*, *57*(2), 258–64. https://doi.org/10.1194/jlr.M064469
Lisé, M.-F., & El-Husseini, A. (2006). The neuroligin and neurexin families: from structure to function at the synapse. *Cellular and Molecular Life Sciences*, *63*(16), 1833–1849. https://doi.org/10.1007/s00018-006-6061-3
Lynch, M. A. (2004). Long-term potentiation and memory. *Physiological Reviews*, *84*(1), 87–136. https://doi.org/10.1152/physrev.00014.2003
Mahley, R. W. (2016). Central Nervous System Lipoproteins: ApoE and Regulation of Cholesterol Metabolism. *Arteriosclerosis, Thrombosis, and Vascular Biology*, *36*(7), 1305–15. https://doi.org/10.1161/ATVBAHA.116.307023
Malenka, R. C., Kauer, J. A., Perkel, D. J., Mauk, M. D., Kelly, P. T., Nicoll, R. A., & Waxham, M. N. (1989). An essential role for postsynaptic calmodulin and protein kinase activity in long-term potentiation. *Nature*, *340*(6234), 554–557. https://doi.org/10.1038/340554a0
Mantych, K. B., & Ferreira, A. (2001). Agrin differentially regulates the rates of axonal and dendritic elongation in cultured hippocampal neurons. *The Journal of Neuroscience : The Official Journal of the Society for Neuroscience*, *21*(17), 6802–9. Retrieved from http://www.ncbi.nlm.nih.gov/pubmed/11517268
Matsumoto-Miyai, K., Sokolowska, E., Zurlinden, A., Gee, C. E., Lüscher, D., Hettwer, S., … Sonderegger, P. (2009). Coincident Pre- and Postsynaptic Activation Induces Dendritic Filopodia via Neurotrypsin-Dependent Agrin Cleavage. *Cell*, *136*(6), 1161–1171. https://doi.org/10.1016/j.cell.2009.02.034
McCroskery, S., Bailey, A., Lin, L., & Daniels, M. P. (2009). Transmembrane agrin regulates dendritic filopodia and synapse formation in mature hippocampal neuron cultures. *Neuroscience*, *163*(1), 168–79. https://doi.org/10.1016/j.neuroscience.2009.06.012
Molinari, F., Rio, M., Meskenaite, V., Encha-Razavi, F., Augé, J., Bacq, D., … Colleaux, L. (2002). Truncating Neurotrypsin Mutation in Autosomal Recessive Nonsyndromic Mental Retardation. *Science*, *298*(5599), 1779–1781. https://doi.org/10.1126/science.1076521
Neumann, F. R., Bittcher, G., Annies, M., Schumacher, B., Krö, S., & Ruegg, M. A. (n.d.). An Alternative Amino-Terminus Expressed in the Central Nervous System Converts Agrin to a Type II Transmembrane Protein. https://doi.org/10.1006/mcne.2000.0932
Neuroscience - Block IV Flashcards | Memorang. (n.d.). Retrieved December 8, 2017, from https://www.memorangapp.com/flashcards/147921/Neuroscience+-+Block+IV/
Nicoll, R. A., & Malenka, R. C. (1999). Expression mechanisms underlying NMDA receptor-dependent long-term potentiation. *Annals of the New York Academy of Sciences*, *868*, 515–25. Retrieved from http://www.ncbi.nlm.nih.gov/pubmed/10414328
Ohno, T., Hasegawa, T., Tsuruoka, T., Terabe, K., Gimzewski, J. K., & Aono, M. (2011). Short-term plasticity and long-term potentiation mimicked in single inorganic synapses. *Nature Materials*, *10*(8), 591–595. https://doi.org/10.1038/nmat3054

Okano, H., Hirano, T., & Balaban, E. (2000). Learning and memory. *Proceedings of the National Academy of Sciences of the United States of America*, *97*(23), 12403–4. https://doi.org/10.1073/pnas.210381897

Ramseger, R., White, R., & Kröger, S. (2009). Transmembrane form agrin-induced process formation requires lipid rafts and the activation of Fyn and MAPK. *The Journal of Biological Chemistry*, *284*(12), 7697–705. https://doi.org/10.1074/jbc.M806719200

Regehr, W. G. (2012). Short-term presynaptic plasticity. *Cold Spring Harbor Perspectives in Biology*, *4*(7), 1–19. https://doi.org/10.1101/cshperspect.a005702

Reist, N. E., Magill, C., & McMahan, U. J. (1987). Agrin-like molecules at synaptic sites in normal, denervated, and damaged skeletal muscles. *Journal of Cell Biology*, *105*(6 I), 2457–2469. https://doi.org/10.1083/jcb.105.6.2457

Riedel, G., & Micheau, J. (2001). Function of the hippocampus in memory formation: desperately seeking resolution. *Progress in Neuro-Psychopharmacology and Biological Psychiatry*, *25*(4), 835–853. https://doi.org/10.1016/S0278-5846(01)00153-1

Rupp, F., Payan, D. G., Magill-Solc, C., Cowan, D. M., & Scheller, R. H. (1991). Structure and expression of a rat agrin. *Neuron*, *6*(5), 811–23. https://doi.org/10.1016/0896-6273(91)90177-2

Singhal, N., & Martin, P. T. (2011). Role of extracellular matrix proteins and their receptors in the development of the vertebrate neuromuscular junction. *Developmental Neurobiology*, *71*(11), 982–1005. https://doi.org/10.1002/dneu.20953

Squire, L. R. (2009). *Encyclopedia of neuroscience*. Academic Press. Retrieved from https://books.google.de/books?id=qX4KAQAAQBAJ&pg=RA4-PA547&lpg=RA4-PA547&dq=The+Schaffer+collaterals+causes+plasticity+in+hippocampus+which+plays+a+considerable+role+in+aspects+of+memory+an+learning&source=bl&ots=4RaK2XYyqg&sig=qN3f1tiZ3jUe3jCLENxs5iXejmE&hl=en&sa=X&ved=0ahUKEwjov_PKmOzXAhXSZFAKHbhcBDwQ6AEIVzAI#v=onepage&q=The Schaffer collaterals causes plasticity in hippocampus which plays a considerable role in aspects of memory an learning&f=false

Stephan, A., Mateos, J. M., Kozlov, S. V, Cinelli, P., Kistler, A. D., Hettwer, S., … Sonderegger, P. (2008). Neurotrypsin cleaves agrin locally at the synapse. *FASEB Journal : Official Publication of the Federation of American Societies for Experimental Biology*, *22*(6), 1861–73. https://doi.org/10.1096/fj.07-100008

Syndecan-3-Deficient Mice Exhibit Enhanced LTP and Impaired Hippocampus-Dependent Memory. (2002). *Molecular and Cellular Neuroscience*, *21*(1), 158–172. https://doi.org/10.1006/MCNE.2002.1167

Tidow, H., Aperia, A., & Nissen, P. (2010). How are ion pumps and agrin signaling integrated? *Trends in Biochemical Sciences*, *35*(12), 653–9. https://doi.org/10.1016/j.tibs.2010.05.004

Wlodarczyk, J., Mukhina, I., Kaczmarek, L., & Dityatev, A. (2011). Extracellular matrix molecules, their receptors, and secreted proteases in synaptic plasticity. *Developmental Neurobiology*, *71*(11), 1040–1053. https://doi.org/10.1002/dneu.20958

Yamaguchi, Y. (2002). Glycobiology of the synapse: the role of glycans in the formation, maturation, and modulation of synapses. *Biochimica et Biophysica Acta*, *1573*(3), 369–76. https://doi.org/10.1016/S0304-4165(02)00405-1

Yang, Y., & Calakos, N. (2013). Presynaptic long-term plasticity. *Frontiers in Synaptic Neuroscience*, *5*, 8. https://doi.org/10.3389/fnsyn.2013.00008

Zito, K., Knott, G., Shepherd, G. M. G., Shenolikar, S., & Svoboda, K. (2004). Induction of Spine Growth and Synapse Formation by Regulation of the Spine Actin Cytoskeleton. *Neuron*, *44*(2), 321–334. https://doi.org/10.1016/J.NEURON.2004.09.022

7. APPENDIX

I. EQUIPMENTS AND DEVICES

Table 1: Devices used during this thesis.

Instruments	Sources
<u>Centrifuges</u> Mega centrifuge Mini centrifunge Benchtop Centrifuge	 Eppendorf AG, Hambug, Germany UltraCruz® Andreas Hettich GmbH & Co.KG, Tuttlingen, Germany
<u>Shakers & Incubators</u> Incubator Shaker CO2/Cell culture Incubator	 Labnet International, Edison, NJ, United states New Brunswick scientific, Edison, NJ, United states Binder GmbH,Tuttlingen, Germany Labotect GmbH, Göttingen, Germany
<u>PCR cyclers</u> PCR machine Real-Time PCR (qPCR) machine	 Biometra GmbH, Göttingen, Germany Roche AG, Basel, Switzerland &Thermo Fisher Scientific Inc, Rochester, NY, United states
<u>Instruments and devices for gel</u> Mini power pack Chamber Benchtop transilluminar	 Biometra GmbH, Göttingen, Germany Biometra GmbH, Göttingen, Germany VWR® international, Pennsylvania, United states
<u>Water bath</u> Water bath Bead bath	 Julabo Labortechnik, Seelbach, Germany Thermo Fisher scientific Inc, Rochester, NY, United states
<u>Microscopes</u> Light microscope Confocal microscope	 Olympus, Shinjuku, Tokyo, Japan Carl Zeiss AG, Jena, Germany
<u>Other instruments & dvices</u> ThermoMix Benchtop pH meter Autoclave Analytical lab scale	 Hangzhou Bioer Technology Co. Ltd. (BIOER), Zhejiang, China IKA-Werke GmbH & Co.KG, Staufen, Germany Systec GmbH, Münster, Germany Sartorius AG, Göttingen, Germany

Vortex	IKA-Werke GmbH & Co.KG, Staufen, Germany
Magnetic stirrer	IKA-Werke GmbH & Co.KG, Staufen, Germany
Nanodrop 2000C	Thermo Fisher scientific Inc, Rochester, NY, United states
Vaccum	Sigma-Aldrich Co. Ltd, Missouri, United states
Laminar flow hood	Thermo Fisher Scientific Inc, Rochester, NY, United states

II. Softwares & webtools

Table 2 : Softwares and webtooles used during this thesis.

Softwares & Webtools	Source
ApE	Utah Biology
Image J	National Institute of health(NIH)
Zen	Carl Zeiss
qPCR program Thermo Fisher scientific & Lightcycler	Thermo Fisher Scientific Roche

III. Media,Buffer and chemicals

Media,Buffer and chemicals used in this thesis.

1. Media

Table 3 : Prepared/ ready to use media used during this thesis.

Media	Components for preparation 1 liter
LB Liquid media	5 g NaCl 10 g tryptone/peptone 5 g yeast extract
LB-Ampicillin agarplates	5 g NaCl 10 g tryptone/peptone 5 g yeast extract 15 g agar 1 ml Ampicillin (100mg/ml)

ψ-broth Media	5 g yeast extract 20 g Trypton 0.75 g KCL 5 g $MgSO_4$($MgSO_{4x7}H_2O$ 10.27g)
Iscove's Modified Dulbecco's Medium	Additives: 50 ml 5-10% Fetal bovine serum 10 ml L-Glutamine
DMEM+	Additives for 50 ml: 48 ml DMEM 1 ml B27 500 µl L-Glutamine 500 µl Penicillin/Streptomycin
Neurobasal+	Additives for 50 ml: 48 ml Neurobasal 1 ml B27 500 µl L-Glutamine 500 µl Penicillin/Streptomycin
Conditional Media	Astrocyte culture in astrocyte growth media 50 ml NB+ 1 ml B27 500 µl L-Glutamine 500 µl Penicillin/Streptomycin

2. Buffer and Stock solutions

Tabel 4 : Buffer and Stock solutions used in this thesis.

Buffers	Components
10% TAE buffer	242g/L TRIS 18.6 g/L EDTA 5.71% (v/v) Acetic acid
<u>Virus production buffers & solutions:</u> Buffer A Wash buffer 1 Wash buffer 2	 Tris 20mM NaCl 150mM Tris 20mM NaCl 100mM Tris 20 mM NaCl 200mM

Elution buffer Solution A Solution B	Tris 20 mM NaCl 400mM 500mM Calcium Chloride 140mM Sodium Chloride 50mM HEPES 1.5mM Di-sodium hydrogen phosphate
<u>Competent cells preparation buffers:</u> Transfection buffer 1 (Tfb 1), pH5.8 Transfection buffer 2 (Tfb 2). pH 6.0	30mM K-Acetate 100mM RbCl 50mM $CaCl_2x2H_2O$ 50mM $MnCl_2x4H_2O$ 15%(v/v) & Filter sterilization 10mM PIPES 75mM $CaCl_2x2H_2O$ 10mM RbCl 5%(v/v) & Filter sterilization
<u>Immunocytochemistry buffer:</u> Permeabilization buffer Blocking buffer	 10% Triton 100X Phosphate buffer saline 1% Normal Goat Serum 1% Tween 20 1% Glycin Phosphate buffer Saline
Ethanol 100%	100%(v/v) ethanol

3. Chemicals

Table 5 : Chemicals used in this thesis.

Name	Source
<u>DNA ladders:</u> 1kb Plus DNA ladder PAN ladder 5x100 lanes HyperladderI	 Cleaver scientific Ltd, Rugby CV22 7DH, UK Pan-Biotec GmbH, Aidenbach, Germany Bioline, Luckenwalde, Germany
Agar-agar LB medium	Carl Roth GmbH, Karlsruhe, Germany Carl Roth GmbH, Karlsruhe, Germany
Agarose	Carl Roth GmbH, Karlsruhe, Germany
Deoxythymidine triphosphate (dTTP) Deoxyguanosine triphosphate (dGTP)	Thermo Scientific - Germany GmbH, Germany

Deoxycytidine triphosphate (dCTP) Deoxyadenosine triphosphate (dATP)	
5x DNA loading dye	Thermo Scientific- Germany GmbH, Germany
SYBR® safe DNA Gel-stain	Invitrogen by Thermo Fisher Scientific, California, United states
TRIS	Sigma-Aldrich Chemie GmbH, Germany
Triton X-100	Carl Roth GmbH, Karlsruhe, Germany
Tween 20	Carl Roth GmbH, Karlsruhe, Germany
Normal Goat Serum	Abcam, Cambridge, United kingdom
Glycin	Carl Roth GmbH, Karlsruhe, Germany
Polyethylenimine 0.1%	Sigma-Aldrich Chemie GmbH, Germany
Paraformaldehyde 4%	Carl Roth GmbH, Karlsruhe, Germany
Endotoxin-free Sodium acetate	Sigma-Aldrich Chemie GmbH, Germany
2-Propanol ROTISOLV	Carl Roth GmbH, Karlsruhe, Germany
TaqMan™	Applied biosystem, California, United states
Fluoromount™ Aqueous Mounting Medium	Sigma-Aldrich Chemie GmbH, Germany
Sodium Chloride Rubidium Chloride Calcium Chloride Mangenase Chloride Glycerol PIPES Yeast extract Trypton Potasium Chloride Ampicillin	Carl Roth GmbH, Karlsruhe, Germany Carl Roth GmbH, Karlsruhe, Germany Carl Roth GmbH, Karlsruhe, Germany Carl Roth GmbH, Karlsruhe, Germany Carl Roth GmbH, Karlsruhe, Germany Carl Roth GmbH, Karlsruhe, Germany Carl Roth GmbH, Karlsruhe, Germany Carl Roth GmbH, Karlsruhe, Germany Carl Roth GmbH, Karlsruhe, Germany Carl Roth GmbH, Karlsruhe, Germany

IV. Enzymes

1. Restriction enzyme

Table 6 : Restriction enzymes.

Restriction enzyme	Recognition sequence	Concentrations	Source
Xhol FD	C^TCGAC	10U/µl	Thermo Scientific-Germany GmbH, Germany
EcoRI FD	G^AATTC	10U/µl	Thermo Scientific-Germany GmbH, Germany
BshTI (AgeI)	A^CCGGT	10U/µl	Thermo Scientific-Germany GmbH, Germany
XbaI	T^CTAGA	10U/µl	Thermo Scientific-Germany GmbH, Germany

2. **Other enzymes**

Table 7 : Other enzymes used for various purposes.

Name	Type	Concentration	Source
Q5® DNA polymerase	Polymerase	5U/µl	New England Biolab, Massachusetts, United states
Q5® Hot Start High-Fidelity DNA Polymerase	Polymerase	5U/µl	New England Biolab, Massachusetts, United states
Bensonase Nuclease	Nuclease	250U/µl	Sigma-Aldrich Chemie GmbH, Germany
T4 DNA ligase	Ligase	5U/µl	Thermo Scientific-Germany GmbH, Germany
Proteinase K	Proteinase	250U/µl	Sigma-Aldrich Chemie

V. Antibodies

The primary and secondary antibodies used in immunocytochemistry in table 11 and 12, respectively.

Table 8 : Primary antibodies.

Primary Antibodies against	Supplier	Species	Dilution
HomerI	Synaptic systems,Göttingen,Germany	Mouse, Monoclonal	1:1000
VglutI	Synaptic systems,Göttingen,Germany	Guinea pig, Polyclonal	1:500
MAP2	Abcam,Cambridge,United Kingdom	Chicken, Polyclonal	1:2000

Table 9 : Secondary antibodies.

Secondary Antibodies against	Supplier	Species	Label	Dilution
Mouse	Life technologies,California,United states	Goat	Alexa Flour 405	1:500
Guinea pig	Life technologies,California,United states	Goat	Alexa Flour 633	1:500
Chicken	Life technologies,California,United states	Goat	Alexa Flour 488	1:1000

Table 10 : Components of the PCR reactions.

Components	Volume
Q5® Hot start DNA polymerase and Q5® DNA polymerase	0.5 µl
dNTP mix	0.5 µl
Forward primer	2.5 µl
Reverse primer	2.5 µl
GC enhancer (optional)	10 µl
Q5® DNA polymerase buffer	10 µl
Template	Variable*
ddH2O	~50

* Template amount varied according to DNA concentration. 100ng of genomic DNA were used.

Table 11 : Thermocycler conditions.

Step	Temperature	Time	Number of cycles
Initial denaturation	98 °C	30 seconds	
Denaturation	98°C	10 seconds	25-30 Cycles
Annealing*	45-72°C	10 seconds	
Extension	72°C	5 minutes	
Final extension	72°C	2 minutes	
Hold	4°C	∞	

*The annealing temperature varies depend upon the melting temperature of different primer.

Table 12 : Master template for restriction endonuclease reactions.

Components	Volume
Restriction enzyme*	2.5 µl
Template 1 µg	X µl
10X FD or orange buffer*	5µl
ddH2O	Up to 50µl
Total	50 µl

*Depending upon the total volume of the reaction, the amount of restriction enzyme and buffer type varied.